Supplementary Material

A gene expression atlas of embryonic neurogenesis in *Drosophila* reveals complex spatiotemporal regulation of lncRNAs.

Alexandra L. McCorkindale (1, 2, 3)*, Philipp Wahle (1, 2), Sascha Werner (1, 2), Irwin Jungreis (4, 5), Peter Menzel (6, 2), Chinmay J. Shukla (7, 8), Rúben Lopes Pereira Abreu (1, 2), Rafael Irizarry (8), Irmtraud M. Meyer (6, 2, 9), Manolis Kellis (4, 5), John L. Rinn (3, 7), Robert P. Zinzen (1, 2)*

1. Supplementary Materials and Methods

1.1 Fly strains and husbandry

Drosophila melanogaster lines used in this study include

yellow-white	$y^1\ w^{1118}$	(source: BSC# 6598)
*IC::*GFP	$y^1\ w^{1118}$ *; ; P{3xind_1.4::GFP}*	(this study)
IC::dsRed	$y^1\ w^{1118}$ *; P{3xind_1.4::dsRed}*	(this study)
VC::dsRed	$y^1\ w^{1118}$ *; ; P{2xvnd_743::dsRED}*	(Karaiskos et al. 2017)
vnd-lexA/VC:FNLDD	$y^1\ w^{1118}$ *; M{3xvnd-lexA:Cit}*$^{attP\_ZH51C}$ *; P{vnd:FNLDD}*	(Krueger et al., unpublished)
rho-lexA/VC:FNLDD	$y^1\ w^{1118}$ *; M{3xrho-lexA:Cit}*$^{attP\_ZH51C}$ *; P{vnd:FNLDD}*	(Krueger et al., unpublished)

The *IC::GFP* and *IC::dsRed* lines were created by standard P-element transgenesis (Rubin & Spradling 1982) in a $y^1\ w^{1118}$ background. The *ind* enhancer (*ind_1.4*) (Markstein et al. 2004) was cloned using primers (ngctagcgtcgacGCTTCAAAGCTCCGGGAAACG & nctcgagTCTGGGCCTTCGGTCCGAAAATG) flanked with NheI and SalI restriction sites (F primer) and with XhoI (R primer). PCR product was T/A cloned into pCRII-Duo and concatemerized using the compatibly cohesive sites XhoI and SalI. 3x *ind_1.4* constructs were directionally subcloned into the P-element vectors pH-Stinger or pRed-HStinger (Barolo et al. 2004) using NheI and XhoI.

Fly stocks were maintained at 25°C, ~60% relative humidity on standard fly food with 12hr light/dark cycles according to standard procedures. 2-hr embryo collections were done on apple juice agar plates with yeast paste after 3 x 1hr pre-lays in the morning, embryos were then aged for an appropriate amount of time at 25°C and ~60% relative humidity before dechorionation.

1.2 DIV-SortSeq

This protocol incorporates portions from (Hrvatin et al. 2014). All steps after dechorionation were performed on ice, using ice-cold DEPC-treated solutions. Primary and secondary antibodies used in this study are listed in Table S1. RNase-free BSA was obtained from Gemini Bioproducts and is critical for isolation of high-quality RNA.

Embryos were collected, dechorionated, and dissociated into single-cell suspension in 15ml PBS, pH 7.5 using 8-12 strokes with the loose pestle of a glass dounce homogenizer. Large debris was removed via filtration with 2 x 90°-rotated sheets of Miracloth into a 15ml conical vial, followed by centrifugation at 40x*g*, 4°C, 3 min. The supernatant was transferred to a 15ml conical vial, cells were pelleted at 1000x*g*, 4°C, 3 min, washed with 1ml PBS, and fixed with 4% formaldehyde at 4°C, 15min. Cross-linking was stopped with Quench Buffer (2.5M Glycine in PBS). Fixed cells were washed twice with 1ml ice-cold PBS, and stored at 4°C overnight in 1ml RNA*later*™ (Thermo, AM7020). Cells were rehydrated via dilution in 9ml ice-cold PBS, centrifugation at 1000 x*g*, 10min, and washed twice in 1ml ice-cold PBS. Fixed cell suspensions were immunostained under RNase-free conditions with primary antibodies with agitation at

4°C, 1.5-2h in 250*µ*l Stain Buffer (1% BSA (w/v), 0.1% saponin, 1:200 RNase inhibitor in RNase-free PBS). After washing 3x 5 min in 1ml Wash Buffer (0.2% BSA, 0.1% saponin in PBS), cells were incubated with conjugated secondary antibodies with agitation at 4°C, 45 min-1h in 250*µ*l Stain Buffer. After washing 3x 5 min in 1ml Wash Buffer, cells were resuspended in 1ml Sort Buffer (0.5% BSA, 2mM EDTA, 1:500 RNase inhibitor in PBS) and filtered with a 70*µ*m cell strainer. Filtered cells were subjected to FACS purification on the FACSAria II (BD Biosciences) and sorted cells collected in Collection Buffer (2% BSA, 1:100 RNase inhibitor in PBS).

FACS-purified cells were pelleted and resuspended in 200*µ*l Digestion Buffer (5M NaCl, 1M Tris-HCl pH 8.0, 200mM EDTA, 10% SDS, 3.2U Proteinase K, 1:100 RNase inhibitor) and incubated at 50°C, 15min (Proteinase K digestion) followed by 80°C, 15min (reversal of formaldehyde cross-links). Samples were transferred to ice and resuspended in 600*µ*l TRIzol™ LS Reagent (Thermo, 10296028). RNA was isolated using the DirectZol™ RNA MicroPrep Kit (Zymo Research, R2060) according to the manufacturer’s instructions. RNA concentration was measured using the Qubit™ RNA HS Assay kit (Thermo, Q32852) and RNA quality determined using the Agilent RNA 6000 Pico Kit (Agilent, 5067-1513). All RNA-seq libraries were constructed using the NuGEN Ovation *Drosophila* RNA-Seq System with 10 ng – 100 ng total RNA input. Library concentration was quantified using the Qubit™ dsDNA HS Assay (Thermo, Q32854) and quality was determined on a BioAnalyzer™ using Agilent High Sensitivity DNA Kits (Agilent, 5067-4626). All libraries were sequenced on the Illumina HiSeq4000 at a mean depth of 62.5 million 75bp paired-end reads per sample. RNA-seq datasets generated for this study are detailed in Tables S5 and S6. *A detailed, step-wise protocol is available upon request.*

1.3 Nuclear-cytoplasmic fractionation

The cell fractionation procedure incorporates portions from (Pawlicki & Steitz 2008; Bhatt et al. 2012; Rosner & Hengstschläger 2012; Shechner et al. 2015). All steps were performed on ice, using ice-cold DEPC-treated solutions, and all centrifugation steps were performed at 4˚C. Embryos were processed to single-cell suspension as described above for *DIV*-SortSeq, then pelleted and resuspended in Cyto Extract Buffer (20mM Tris pH 7.6, 0.1mM EDTA, 2mM $MgCl_2$). After hypotonic swelling, cells were gently lysed by addition of 0.6% CHAPS for isolation of the cytoplasmic fraction. Nuclei were pelleted at 500x*g* for 5min, and the supernatant retained, and an appropriate volume of TRIzol™ LS Reagent was added (cytoplasmic fraction).

Nuclei were washed with Nuclei Wash Buffer (20mM Tris pH 7.6, 0.1mM EDTA, 2mM $MgCl_2$, 0.6% CHAPS), resuspended in Nuclei Resuspension Buffer (10mM Tris, pH 7.6, 150mM NaCl, 0.15% NP-40) and pelleted at 12,000x*g*, 10min in Sucrose Buffer (10mM Tris, pH 7.5, 150mM NaCl, 24% sucrose). After washing (1mM EDTA in PBS), nuclei pellet was resuspended in TRIzol™ Reagent. RNA was isolated and concentration and quality determined as described for above for *DIV*-SortSeq.

1.4 Quantitative RT-PCR (qPCR)

50ng of total RNA was reverse-transcribed with the QuantiTect Reverse Transcription kit (Qiagen, 205310) in a total volume of 20*µ*l, according to the manufacturer’s instructions. For each gene, 0.2*µ*l cDNA was used for input into qPCR using SensiFAST™ SYBR® No-ROX Kit (Bioline, 98020) and 5*µ*M forward and reverse primers in a total volume of 20*µ*l. qPCR primer sequences are listed in Table S2. qPCR thermal cycling and fluorescent data acquisition was performed using the BioRad CFX96 Touch™ Real-Time PCR Detection System. Expression fold changes were calculated via the $\Delta\Delta C_T$ method (Vandesompele et al. 2002; Schmittgen & Livak 2008), normalized to the mean C_T of two reference genes: *α-tubulin* and *actin 42A*.

1.5 RNA probe design and synthesis for RNA in situ hybridization.

Where available, cDNA clones were obtained from the *Drosophila* Gene Collection or *Drosophila* Genomics Resource Center (Stapleton et al. 2002), detailed in Table S3. Constructs were linearized via restriction digestion, and subjected to *in vitro* transcription using appropriate RNA Polymerases (Roche), using ribonucleotide mixtures containing dUTP-DIG, -FITC, or -Biotin (Roche).

Where cDNA clones were not available, PCR primers were designed to amplify a region within the transcribed locus from genomic DNA. Primer sequences are detailed in Table S4. A T7 promoter sequence appended to the reverse primer allowed *in vitro* transcription directly from the PCR product. After template digest by DNaseI, RNA probes were sheared at 65°C for 3-20 min in carbonation buffer (120mM Na_2CO_3, 80mM $NaHCO_3$, pH 10.2), length of carbonation depended on probe length. RNA probes were precipitated at -20°C overnight and resuspended in Hyb-A Buffer (50% formamide, 5X SSC, 0.1% Tween-20).

2. Supplementary Tables

Table S1: Primary and secondary antibodies used in this study

Target	*Supplier*	*Catalog #*	*Application*	*Antibody Type*	*Conjugate*	*Dilution*
RFP	Thermo	710530	*Primary*	Rabbit polyclonal	N/A	1:500
GFP	Thermo	G10362	*Primary*	Rabbit polyclonal	N/A	1:500
Pros	DSHB	MR1A	*Primary*	Mouse monoclonal	N/A	1:20
Elav	DSHB	9F8A9	*Primary*	Mouse monoclonal	N/A	1:500
Repo	DSHB	8D12	*Primary*	Mouse monoclonal	N/A	1:20
Rabbit IgG	Thermo	A21428	*Secondary*	Goat polyclonal	*Alexa Fluor 555*	1:500
Mouse IgG	Thermo	A32727	*Secondary*	Goat polyclonal	*Alexa Fluor 555*	1:500

Table S2: qPCR primer sequences

Target	*Forward primer*	*Reverse primer*	*Size (bp)*
α-Tubulin	TGTCGCGTGTGAAACACTTC	AGCAGGCGTTTCCAATCTG	585
Actin 42A	GCGTCGGTCAATTCAATCTT	AAGCTGCAACCTCTTCGTCA	292
Prospero	CGGCATGGCTCCTACTTCTT	TAGCGCACCCAGAAGAACAT	78
Worniu	ATGGATAAACTCAAGTACAGCCG	AAGTCCACTGGTCCTTCATCA	107
Elav	ACGCTCCTGCCACAGAAAAA	CGTCGCCGTATTTCGCTC	211
Lim3	GATGGAGGATCGTAAGCTGATCT	GTAGGCCGTTTTCAGGGTCTC	154
Repo	CTCCGCCAAGTAGTTCCTCC	AGGCAGTAAAGGTGGTTCTCG	216
Gcm	ACAAGGCCAGAAGGAAGCAG	CAAGCCTGGATTTCCAAGCGA	76

Table S3: List of commercially-available cDNA clones for RNA probe synthesis

RNA target	*DGRC Reference #*
ind	RT01026
vnd	PCSP6029
pros	LD37627
elav	LD33076-IR
repo	GH05443-dg
CR30009	RE30084
CR32730	RE54940
CR32111	RE52337

Table S4: PCR primer sequences for RNA probe synthesis

Target	*Forward primer*	*T7 promoter + Reverse primer*	*Size (bp)*
CR46003	TGTGTCGCACAGGATGTGT	TAATACGACTCACTATAGGGTGCTGGCGGGGAAATTATGT	908
cherub	CGAGGAACCTTCGGTGCATA	TAATACGACTCACTATAGGGGCTTGGGTGATTTCGAGGGA	1511
CR44024	GTGTCGTGTCGGGTAAGTGT	TAATACGACTCACTATAGGGAAGTGGCCTGTCTCAGAACG	1268
CR32111	GTATGCGCTCGAACTCGGTAA	TAATACGACTCACTATAGGGGCCGGCATGAGCAAACACAAA	1232

148 *Table S5: Summary of RNA-seq datasets – DIV-SortSeq*

Sample name	***Fly line***	***Target protein***	***Cell Type***	***Enriched/depleted***	***Time point***	***Replicate***	***# reads (M)***
4-6h_Ind-neg_1	*IC*::dsRed	dsRed	Intermediate column	Depleted	4-6h	1	89.9
4-6h_Ind-neg_2	*IC*::dsRed	dsRed	Intermediate column	Depleted	4-6h	2	140.1
4-6h_Ind-pos_1	*IC*::dsRed	dsRed	Intermediate column	Enriched	4-6h	1	76.2
4-6h_Ind-pos_2	*IC*::dsRed	dsRed	Intermediate column	Enriched	4-6h	2	81.6
4-6h_Vnd-neg_1	*VC*::dsRed	dsRed	Ventral column	Depleted	4-6h	1	62.6
4-6h_Vnd-neg_2	*VC*::dsRed	dsRed	Ventral column	Depleted	4-6h	2	64.3
4-6h_Vnd-pos_1	*VC*::dsRed	dsRed	Ventral column	Enriched	4-6h	1	61.4
4-6h_Vnd-pos_2	*VC*::dsRed	dsRed	Ventral column	Enriched	4-6h	2	65.6
4-6h_Pros-neg_1	*vnd*-lexA/VC:FNLDD	Prospero	Neuroblasts	Depleted	4-6h	1	59.8
4-6h_Pros-neg_2	*vnd*-lexA/VC:FNLDD	Prospero	Neuroblasts	Depleted	4-6h	2	79.1
4-6h_Pros-pos_1	*vnd*-lexA/VC:FNLDD	Prospero	Neuroblasts	Enriched	4-6h	1	61.9
4-6h_Pros-pos_2	*vnd*-lexA/VC:FNLDD	Prospero	Neuroblasts	Enriched	4-6h	2	59.1
6-8h_Ind-neg_1	*IC*::GFP	GFP	Intermediate column	Depleted	6-8h	1	61
6-8h_Ind-neg_2	*IC*::GFP	GFP	Intermediate column	Depleted	6-8h	2	59.9
6-8h_Ind-pos_1	*IC*::GFP	GFP	Intermediate column	Enriched	6-8h	1	57
6-8h_Ind-pos_2	*IC*::GFP	GFP	Intermediate column	Enriched	6-8h	2	70.9
6-8h_Vnd-neg_1	*VC*::dsRed	dsRed	Ventral column	Depleted	6-8h	1	73.2
6-8h_Vnd-neg_2	*VC*::dsRed	dsRed	Ventral column	Depleted	6-8h	2	61
6-8h_Vnd-pos_1	*VC*::dsRed	dsRed	Ventral column	Enriched	6-8h	1	61.6
6-8h_Vnd-pos_2	*VC*::dsRed	dsRed	Ventral column	Enriched	6-8h	2	73.9
6-8h_Pros-neg_1	*vnd*-lexA/VC:FNLDD	Prospero	Neuroblasts	Depleted	6-8h	1	64.5
6-8h_Pros-neg_2	*vnd*-lexA/VC:FNLDD	Prospero	Neuroblasts	Depleted	6-8h	2	76.6
6-8h_Pros-pos_1	*vnd*-lexA/VC:FNLDD	Prospero	Neuroblasts	Enriched	6-8h	1	54.3
6-8h_Pros-pos_2	*vnd*-lexA/VC:FNLDD	Prospero	Neuroblasts	Enriched	6-8h	2	58.8
6-8h_Elav-neg_1	*IC*::GFP	Elav	Neurons	Depleted	6-8h	1	62.2
6-8h_Elav-neg_2	*yw*	Elav	Neurons	Depleted	6-8h	2	57.2
6-8h_Elav-pos_1	*IC*::GFP	Elav	Neurons	Enriched	6-8h	1	53.8
6-8h_Elav-pos_2	*yw*	Elav	Neurons	Enriched	6-8h	2	70.4
6-8h_Repo-neg_1	*IC*::GFP	Repo	Glia	Depleted	6-8h	1	59.6
6-8h_Repo-neg_2	*IC*::GFP	Repo	Glia	Depleted	6-8h	2	71.4
6-8h_Repo_pos_1	*IC*::GFP	Repo	Glia	Enriched	6-8h	1	66.6
6-8h_Repo_pos_2	*IC*::GFP	Repo	Glia	Enriched	6-8h	2	56.8
8-10h_Elav-neg_1	*yw*	Elav	Neurons	Depleted	8-10h	1	74.5
8-10h_Elav-neg_2	*yw*	Elav	Neurons	Depleted	8-10h	2	44.1
8-10h_Elav-pos_1	*yw*	Elav	Neurons	Enriched	8-10h	1	69.9
8-10h_Elav-pos_2	*yw*	Elav	Neurons	Enriched	8-10h	2	62.9
8-10h_Repo-neg_1	*vnd*-lexA/VC:FNLDD	Repo	Glia	Depleted	8-10h	1	61.5
8-10h_Repo-neg_2	*vnd*-lexA/VC:FNLDD	Repo	Glia	Depleted	8-10h	2	60.9
8-10h_Repo-pos_1	*vnd*-lexA/VC:FNLDD	Repo	Glia	Enriched	8-10h	1	61.4

8-10h_Repo-pos_2	*vnd*-lexA/VC:FNLDD	Repo	Glia	Enriched	8-10h	2	65.6
18-22h_Elav-neg_1	*vnd*-lexA/VC:FNLDD	Elav	Neurons	Depleted	18-22h	1	68.6
18-22h_Elav-neg_2	*vnd*-lexA/VC:FNLDD	Elav	Neurons	Depleted	18-22h	2	61.9
18-22h_Elav-pos_1	*vnd*-lexA/VC:FNLDD	Elav	Neurons	Enriched	18-22h	1	66
18-22h_Elav-pos_2	*vnd*-lexA/VC:FNLDD	Elav	Neurons	Enriched	18-22h	2	63.9
18-22h_Repo-neg_1	*vnd*-lexA/VC:FNLDD	Repo	Glia	Depleted	18-22h	1	58.3
18-22h_Repo-neg_2	*vnd*-lexA/VC:FNLDD	Repo	Glia	Depleted	18-22h	2	63.4
18-22h_Repo-pos_1	*vnd*-lexA/VC:FNLDD	Repo	Glia	Enriched	18-22h	1	70.5
18-22h_Repo-pos_2	*vnd*-lexA/VC:FNLDD	Repo	Glia	Enriched	18-22h	2	75.9

Table S6: Summary of RNA-seq datasets – Fractionation-Seq

Sample name	***Fly line***	***Fraction***	***Time point***	***Replicate***	***Number of reads (M)***
Cyto_18-22h_1	*rho*-lexA/VC:FNLDD	Cytoplasmic	18-22h	1	163.2
Cyto_18-22h_2	*rho*-lexA/VC:FNLDD	Cytoplasmic	18-22h	2	179.1
Cyto_6-8h_1	*rho*-lexA/VC:FNLDD	Cytoplasmic	6-8h	1	189.3
Cyto_6-8h_2	*rho*-lexA/VC:FNLDD	Cytoplasmic	6-8h	2	179.3
Nuc_18-22h_1	*rho*-lexA/VC:FNLDD	Nuclear	18-22h	1	203
Nuc_18-22h_2	*rho*-lexA/VC:FNLDD	Nuclear	18-22h	2	176.1
Nuc_6-8h_1	*rho*-lexA/VC:FNLDD	Nuclear	6-8h	1	193.9
Nuc_6-8h_2	*rho*-lexA/VC:FNLDD	Nuclear	6-8h	2	193.7
Whole_18-22h_1	*rho*-lexA/VC:FNLDD	Whole embryo	18-22h	1	183.2
Whole_18-22h_2	*rho*-lexA/VC:FNLDD	Whole embryo	18-22h	2	180.7
Whole_6-8h_1	*rho*-lexA/VC:FNLDD	Whole embryo	6-8h	1	197.4
Whole_6-8h_2	*rho*-lexA/VC:FNLDD	Whole embryo	6-8h	2	196.1

2.1 Table S7: All protein-coding ‘computed genes’ correlated (r > 0.9) with neurogenic marker genes in DIV-SortSeq expression data

Flybase ID	*Annotation ID*
FBgn0036725	CG18265
FBgn0034009	CG8155
FBgn0036008	CG3408
FBgn0030017	CG2278
FBgn0264449	CG43867
FBgn0051235	CG31235
FBgn0037166	CG11426
FBgn0032752	CG10702
FBgn0038114	CG11670
FBgn0037206	CG12768
FBgn0032485	CG9426
FBgn0038321	CG6218
FBgn0038720	CG6231
FBgn0033283	CG11635
FBgn0043806	CG32032
FBgn0033287	CG8701
FBgn0031540	CG3238
FBgn0031961	CG7102
FBgn0040984	CG4440
FBgn0026876	CG11403
FBgn0035689	CG7376
FBgn0025388	CG12179
FBgn0036503	CG13454
FBgn0040809	CG13465
FBgn0032489	CG15480
FBgn0041702	CG15107
FBgn0034403	CG18190
FBgn0031070	CG12702
FBgn0250754	CG42232
FBgn0261538	CG42662
FBgn0034514	CG13427
FBgn0036670	CG13029
FBgn0031252	CG13690
FBgn0040346	CG3704
FBgn0039013	CG4813
FBgn0037633	CG9839
FBgn0028506	CG4455
FBgn0037844	CG4570
FBgn0037924	CG14712
FBgn0035464	CG12006
FBgn0027602	CG8611
FBgn0037051	CG10565
FBgn0052756	CG32756
FBgn0036710	CG6479
FBgn0039735	CG7911
FBgn0023515	CG14814
FBgn0033160	CG11107
FBgn0033169	CG11123
FBgn0029672	CG2875
FBgn0025633	CG13366
FBgn0050183	CG30183
FBgn0030768	CG9723
FBgn0025626	CG4281
FBgn0035213	CG2199
FBgn0031403	CG15387
FBgn0043456	CG4747
FBgn0052428	CG32428
FBgn0031062	CG14230
FBgn0035315	CG8960
FBgn0032050	CG13096
FBgn0038552	CG18012
FBgn0031764	CG9107
FBgn0035878	CG7182
FBgn0034073	CG8414
FBgn0033766	CG8771
FBgn0037958	CG6962
FBgn0034447	CG7744
FBgn0035842	CG7504
FBgn0038272	CG7265
FBgn0039544	CG12877
FBgn0033615	CG7741
FBgn0030122	CG16892
FBgn0051365	CG31365
FBgn0052318	CG32318
FBgn0039566	CG4849
FBgn0037746	CG8478
FBgn0030813	CG4949
FBgn0029825	CG12728
FBgn0038768	CG4936
FBgn0037149	CG14561
FBgn0037372	CG2091
FBgn0030915	CG6179
FBgn0027514	CG1024
FBgn0031947	CG7154
FBgn0030660	CG8097
FBgn0036565	CG5235
FBgn0024364	CG11417
FBgn0036994	CG5199
FBgn0033527	CG11777
FBgn0039743	CG7946
FBgn0262719	CG43163
FBgn0036886	CG9300
FBgn0034264	CG10933
FBgn0025627	CG4194
FBgn0032682	CG10176
FBgn0031001	CG7884
FBgn0037213	CG12581
FBgn0038660	CG14291
FBgn0034933	CG3735
FBgn0030855	CG5800
FBgn0035414	CG14965
FBgn0036214	CG7264
FBgn0030317	CG1561
FBgn0036660	CG13025
FBgn0031597	CG17612
FBgn0036483	CG12316
FBgn0032512	CG9305
FBgn0037644	CG11964
FBgn0040385	CG12496
FBgn0033802	CG17724
FBgn0039733	CG11504
FBgn0037504	CG1142
FBgn0036522	CG7372
FBgn0035402	CG12082
FBgn0031769	CG9135
FBgn0038551	CG7357
FBgn0032348	CG4751
FBgn0035987	CG3689
FBgn0037918	CG6791
FBgn0035872	CG7185
FBgn0031529	CG9662
FBgn0031492	CG3542
FBgn0086855	CG17078
FBgn0033990	CG10265
FBgn0032454	CG5787
FBgn0037622	CG8202
FBgn0032751	CG17343
FBgn0266917	CG16941
FBgn0034114	CG4282
FBgn0034750	CG3732
FBgn0030738	CG9915
FBgn0035235	CG7879
FBgn0028474	CG4119
FBgn0085451	CG34422
FBgn0030293	CG1737
FBgn0050020	CG30020
FBgn0029941	CG1677
FBgn0033021	CG10417
FBgn0027503	CG11970
FBgn0032388	CG6686
FBgn0038546	CG7379
FBgn0035481	CG12605
FBgn0260451	CG14042
FBgn0035677	CG13293
FBgn0036202	CG6024
FBgn0035643	CG13287
FBgn0034184	CG9646
FBgn0052105	CG32105
FBgn0031257	CG4133
FBgn0037050	CG10566
FBgn0025712	CG13920
FBgn0027550	CG6495
FBgn0031762	CG9098
FBgn0035246	CG13928
FBgn0039808	CG12071
FBgn0030508	CG15760
FBgn0033960	CG10151
FBgn0030596	CG12398
FBgn0052085	CG32085
FBgn0030012	CG18262
FBgn0030223	CG2111
FBgn0051030	CG31030
FBgn0035903	CG6765
FBgn0030595	CG14406
FBgn0033983	CG10253
FBgn0031955	CG14535
FBgn0033497	CG12912
FBgn0034154	CG5267
FBgn0033872	CG6329
FBgn0030588	CG9521
FBgn0085382	CG34353
FBgn0085218	CG34189
FBgn0030594	CG9509
FBgn0034459	CG16716
FBgn0259823	CG42404
FBgn0032800	CG10137
FBgn0038926	CG13409
FBgn0039064	CG4467
FBgn0259163	CG42268
FBgn0259994	CG42492
FBgn0039030	CG6660
FBgn0036579	CG5027
FBgn0029708	CG3556
FBgn0030586	CG12539
FBgn0038596	CG14312
FBgn0263072	CG43347
FBgn0037525	CG17816
FBgn0030742	CG9919
FBgn0265084	CG44195
FBgn0030592	CG9514
FBgn0262476	CG43066
FBgn0035033	CG3548
FBgn0040351	CG11638
FBgn0028647	CG11902
FBgn0031313	CG5080
FBgn0039915	CG1732
FBgn0029896	CG3168
FBgn0039024	CG4721
FBgn0032897	CG9336
FBgn0034128	CG4409
FBgn0034417	CG15117
FBgn0031816	CG16947
FBgn0030261	CG15203
FBgn0033446	CG1648
FBgn0052354	CG32354
FBgn0031627	CG15630
FBgn0036927	CG7433
FBgn0034618	CG9485
FBgn0083972	CG34136
FBgn0031589	CG3714
FBgn0036760	CG5567
FBgn0032899	CG9338

3. Supplementary Notes

3.1 Column interpretation for File S4: PhyloCSF

Intervals	Intervals of the input transcript
Strand	Strand
TranscriptName	Name from the input bed file
TrUCSCview	Link to show the entire transcript in UCSC browser
ORFintervals	Intervals of the ORF (not including the stop codon)
ORFstart	0-based transcript coordinate of first base of ORF
ORFend	0-based transcript coordinate of last base of ORF
NumCodons	Number of codons in the ORF
PhyloCSF	Raw PhyloCSF score of the ORF
RelBL	Fraction of branch length of the phylogenetic tree spanned by species present in the alignment of this ORF
ScorePerCodon	PhyloCSF divided by NumCodons
PhyloCSFPsi	Length adjusted score, a log likelihood, in decibans
Pval	Probability a region of this length, none-of-which has ever been coding, has this score or higher
CorrectedPvalTr	p-val with Holm-Bonferroni correction for number of ORFs in this transcript
CorrectedPvalAll	p-val with Holm-Bonferroni correction for total number of ORFs
FDR	Benjamini & Hochberg false discovery rate.
LocalFDR	Local FDR (Efron et al. 2001).
AntiScorePerCodon	Score on opposite strand in frame that shares 3rd codon position
ScoreDiff	ScorePerCodon - AntiScorePerCodon
GC	GC content of ORF
CpGratio	Number of CpGs in ORF divided by the expected number based on C and G content
CodAlignView	Link to view ORF alignment in CodAlignView, the Codon Alignment Viewer, with 10-codon context on each side
OrfUCSCview	Link to show the ORF in UCSC browser

4. Supplementary Figures

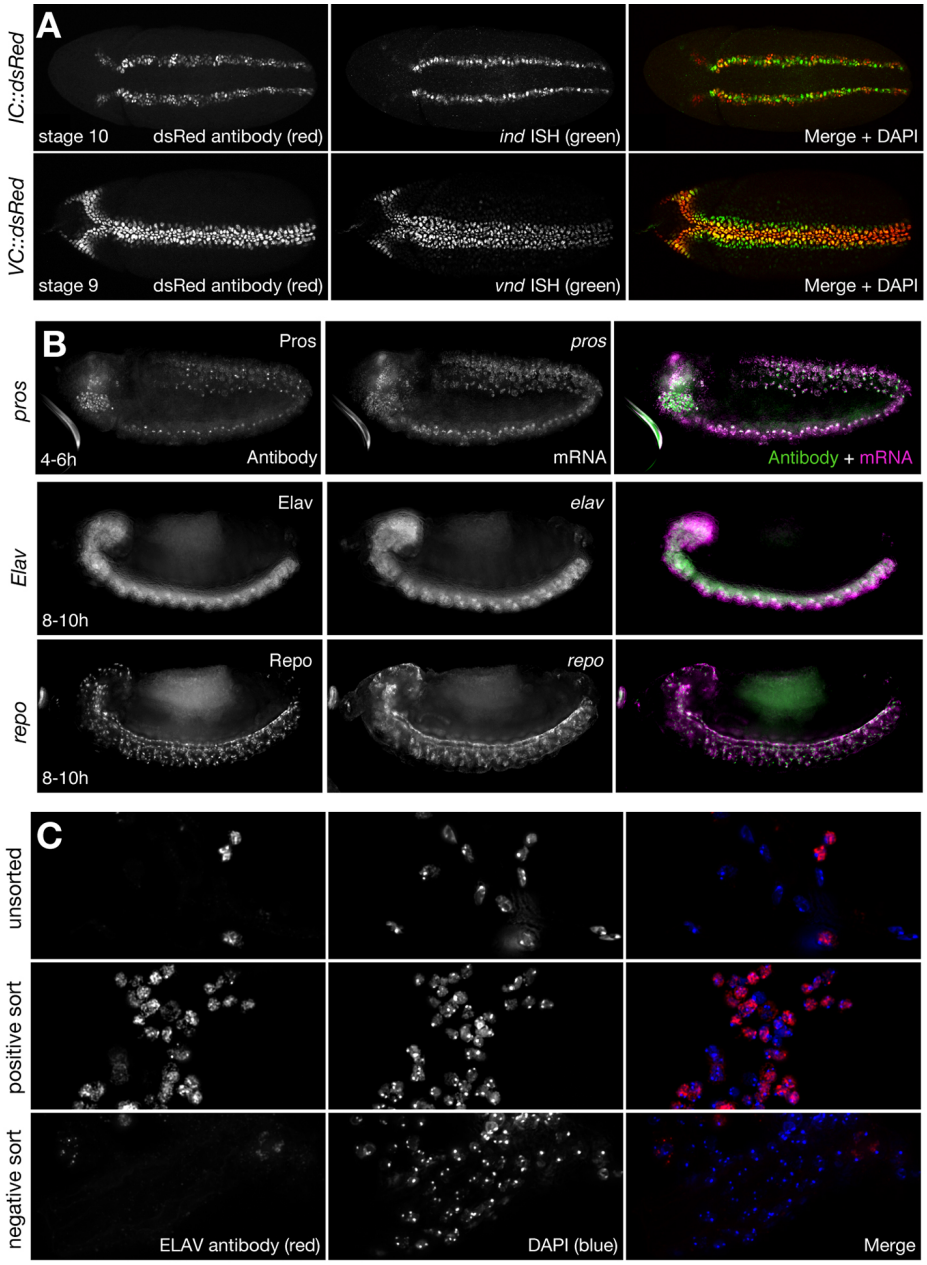

Fig. S1: Neurogenic cell populations can be faithfully marked and purified
(A) Visualization of fluorescent reporter expression in *VC::dsRed* (top panel) and *IC::dsRed* (bottom panel) transgenic embryos. Tissue reporter shown on left and in red by antibody stain, expression of the tissue marker is shown in the middle and in green by *in situ* hybridization. Shown are whole mount embryos, ventral views anterior left. (B) Multiplex whole mount immunohistochemistry (green) and RNA-FISH (magenta) show faithfulness of the antibody sorting markers for neuroblasts (Pros; top panel) at 4-6h, and neurons (Elav; middle panel) and glia (Repo; bottom panel) at 8-10h. (C) Immunohistochemical staining of endogenous Elav protein in cells of dissociated embryos pre- and post-FACS.

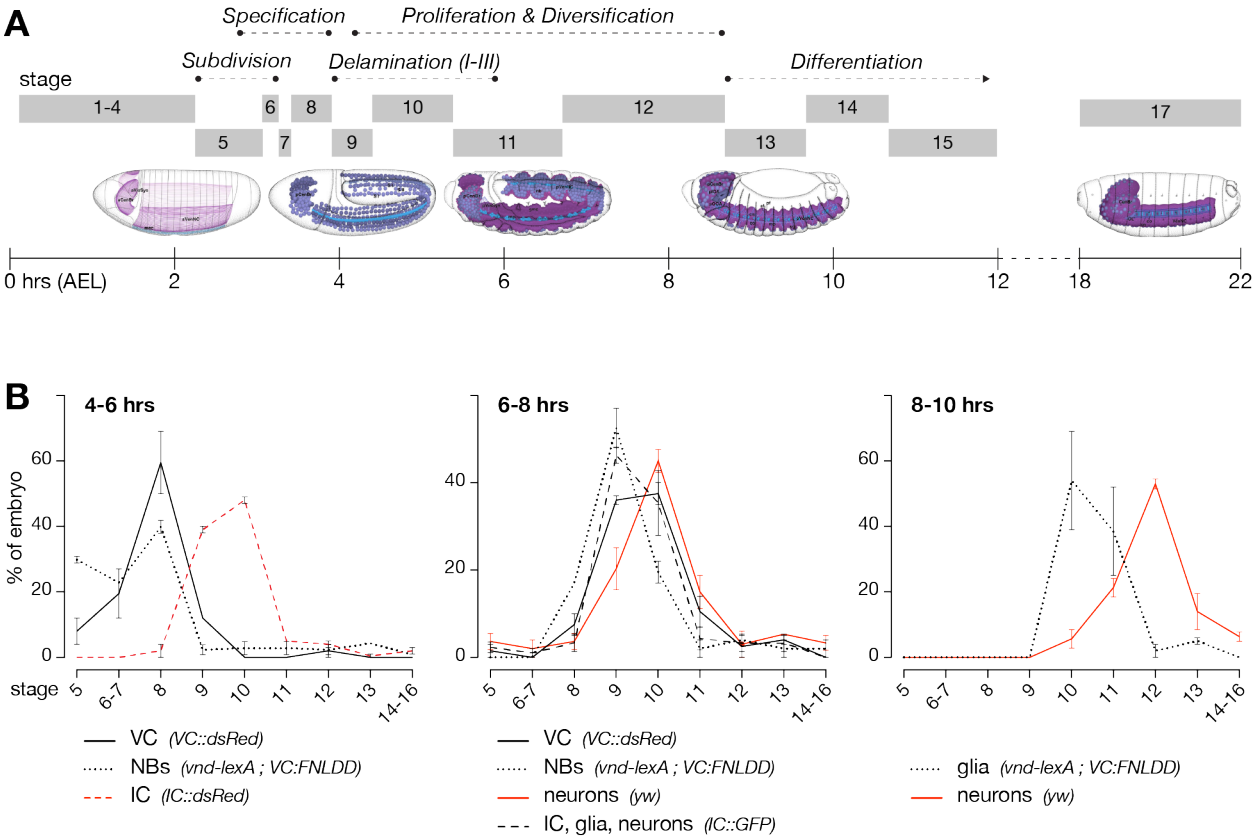

Fig. S2: Timed embryo collections encompass major neurogenic events

(A) Overview of *Drosophila* embryonic neurogenesis, timing and stages. Embryo images show stages of neurogenesis schematically and were obtained from the *Atlas of Drosophila Development* by Volker Hartstein (CSHL Press, 1992, used with permission). (B) Staging of representative samples corresponding to timed embryo collections (n = 2-3 collections per line). Staging according to (Campos-Ortega & Hartenstein 1985). Cell type markers targeted for *DIV*-MARIS indicated for each fly line.

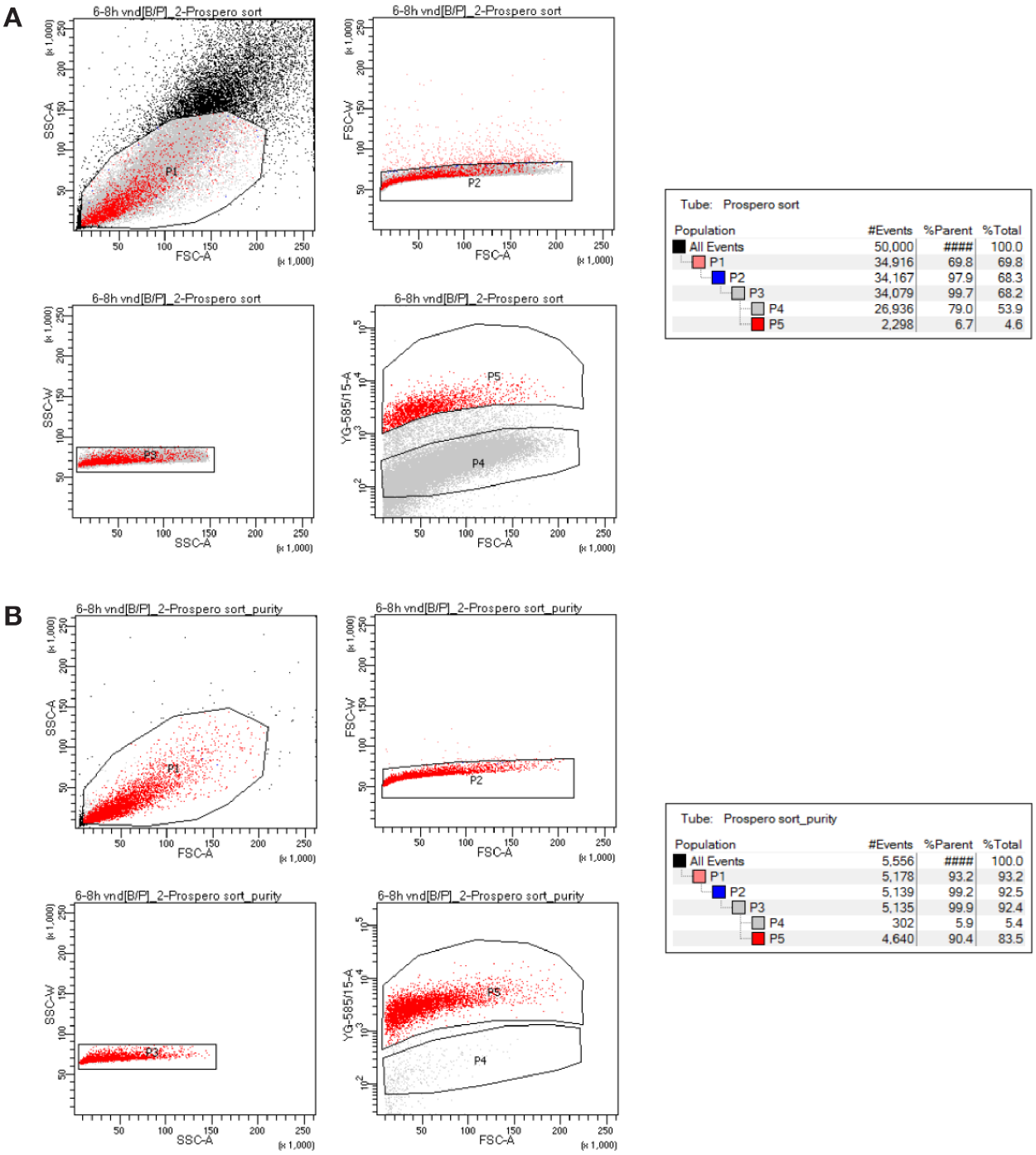

Fig. S3: FACS gating strategy yields high purity of sorted populations
(A) Example FACS gating strategy for sorting of marker-positive (P5; 6.7%) and marker-negative cells (P4; 79%). (B) Re-sort of marker-positive sorted cells shows enrichment of marker-positive (P5; 90.4%) and depletion of marker-negative cells (P4; 5.9%).

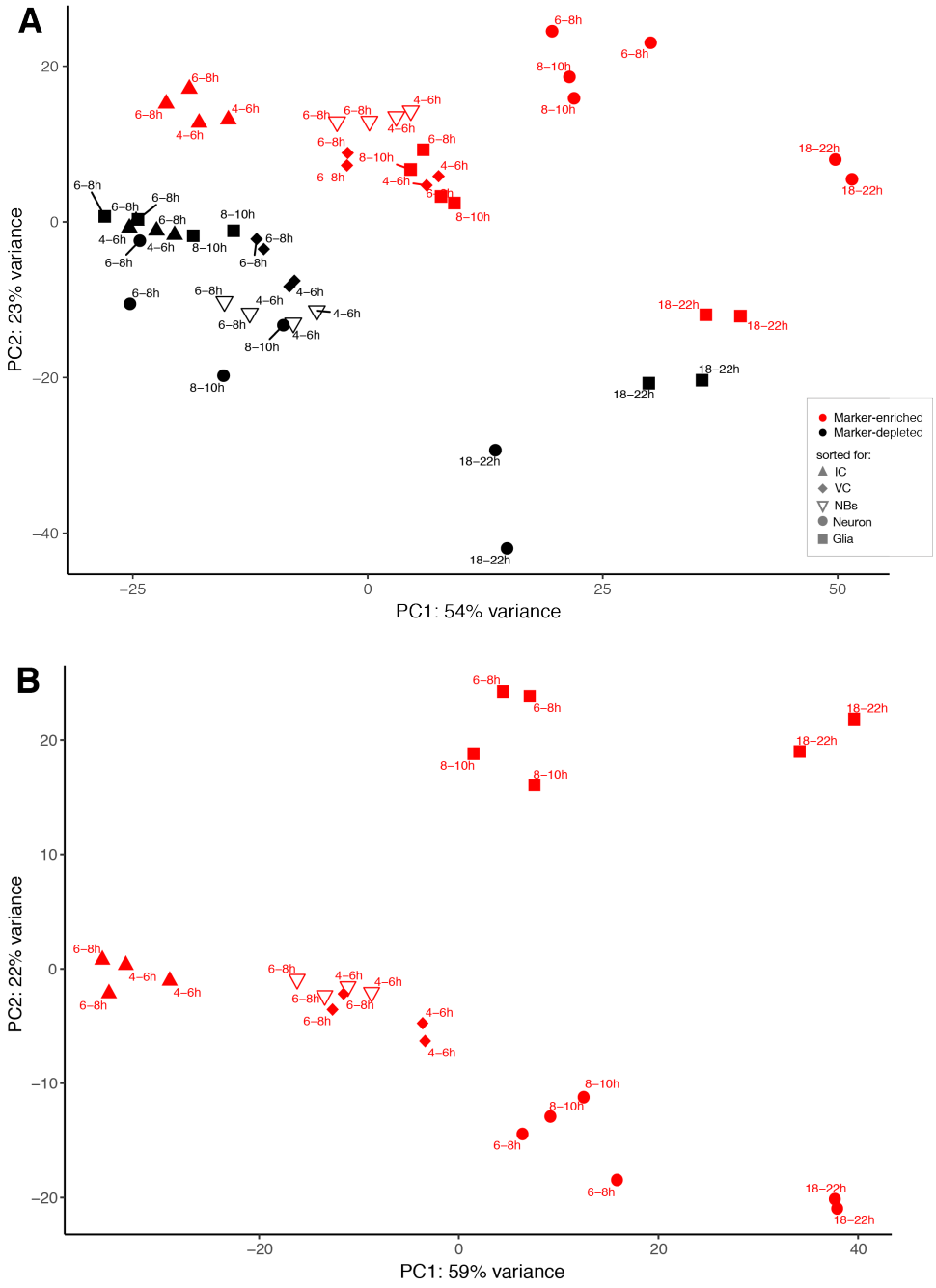
A
PC2: 23% variance
PC1: 54% variance
Marker-enriched
Marker-depleted
sorted for:
IC
VC
NBs
Neuron
Glia
B
PC2: 22% variance
PC1: 59% variance

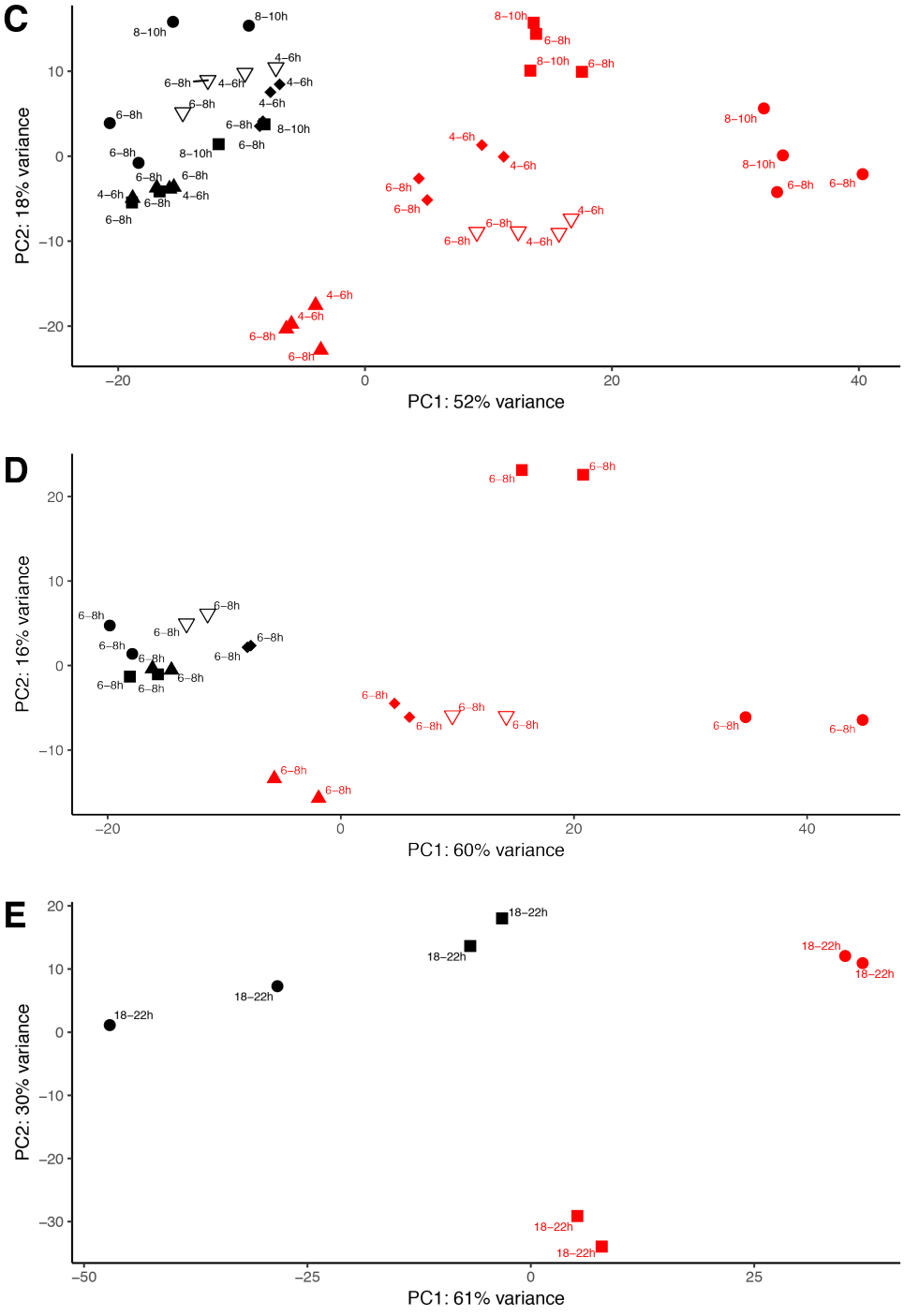
C
PC2: 18% variance
PC1: 52% variance
D
PC2: 16% variance
PC1: 60% variance
E
PC2: 30% variance
PC1: 61% variance

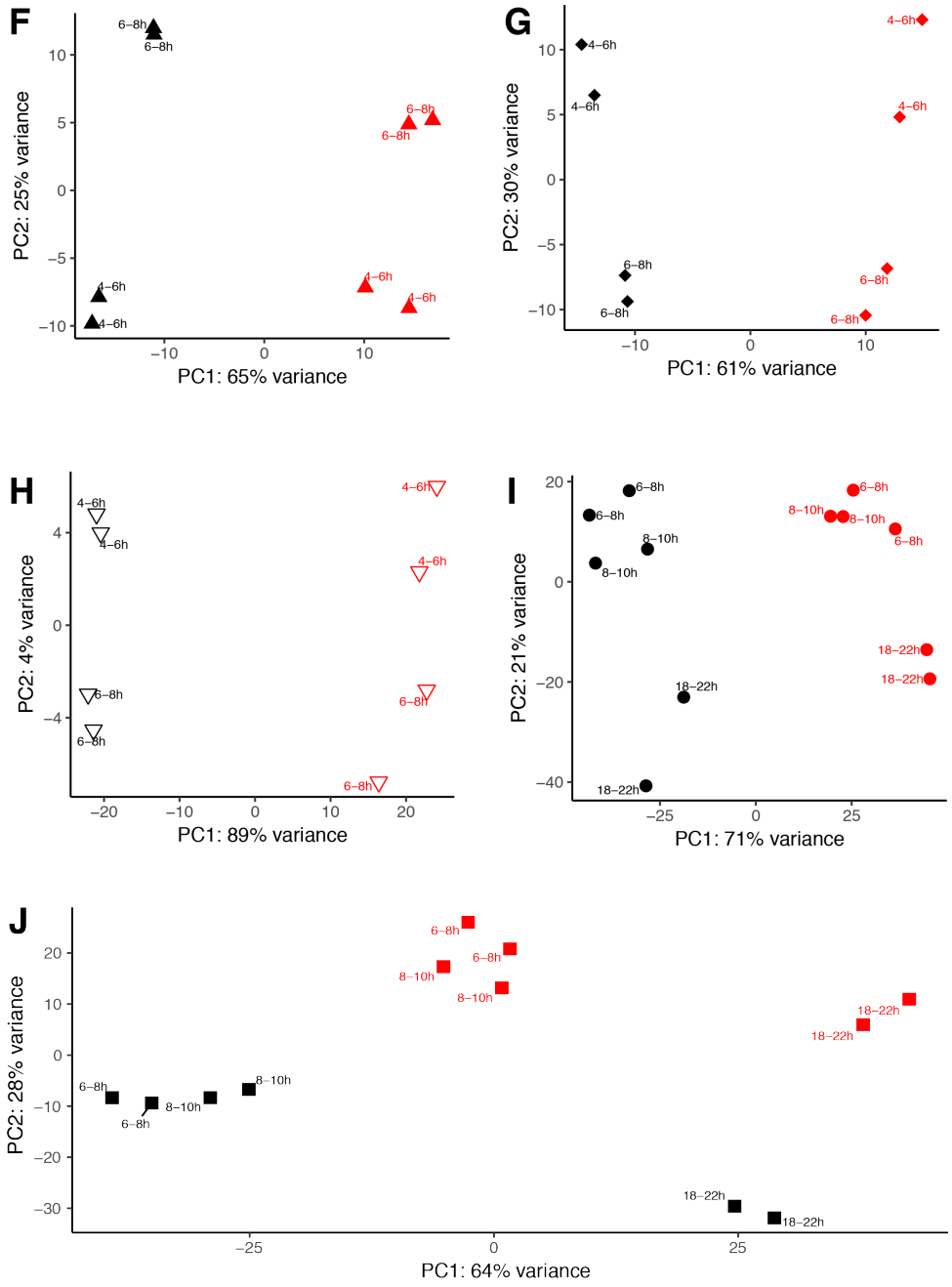

Fig. S4: Principal component analyses separate spatiotemporal transcriptomes according to tissue and developmental age

Principal Component Analysis (PCA) with multiple permutations of datasets generated by *DIV*-SortSeq. Marker-enriched datasets depicted in red, marker-depleted datasets in black. (A) All datasets. (B). Only marker-positive datasets. (C). Only early (4-6, 6-8, 8-10h) datasets. (D) Only 6-8h datasets. (E). Only 18-22h datasets. (F). Only datasets sorted for *ind* expression. (G). All datasets sorted for *vnd* expression. (H) All datasets sorted for *pros* expression. (I) All datasets sorted for *elav* expression. (J) All datasets sorted on *repo* expression.

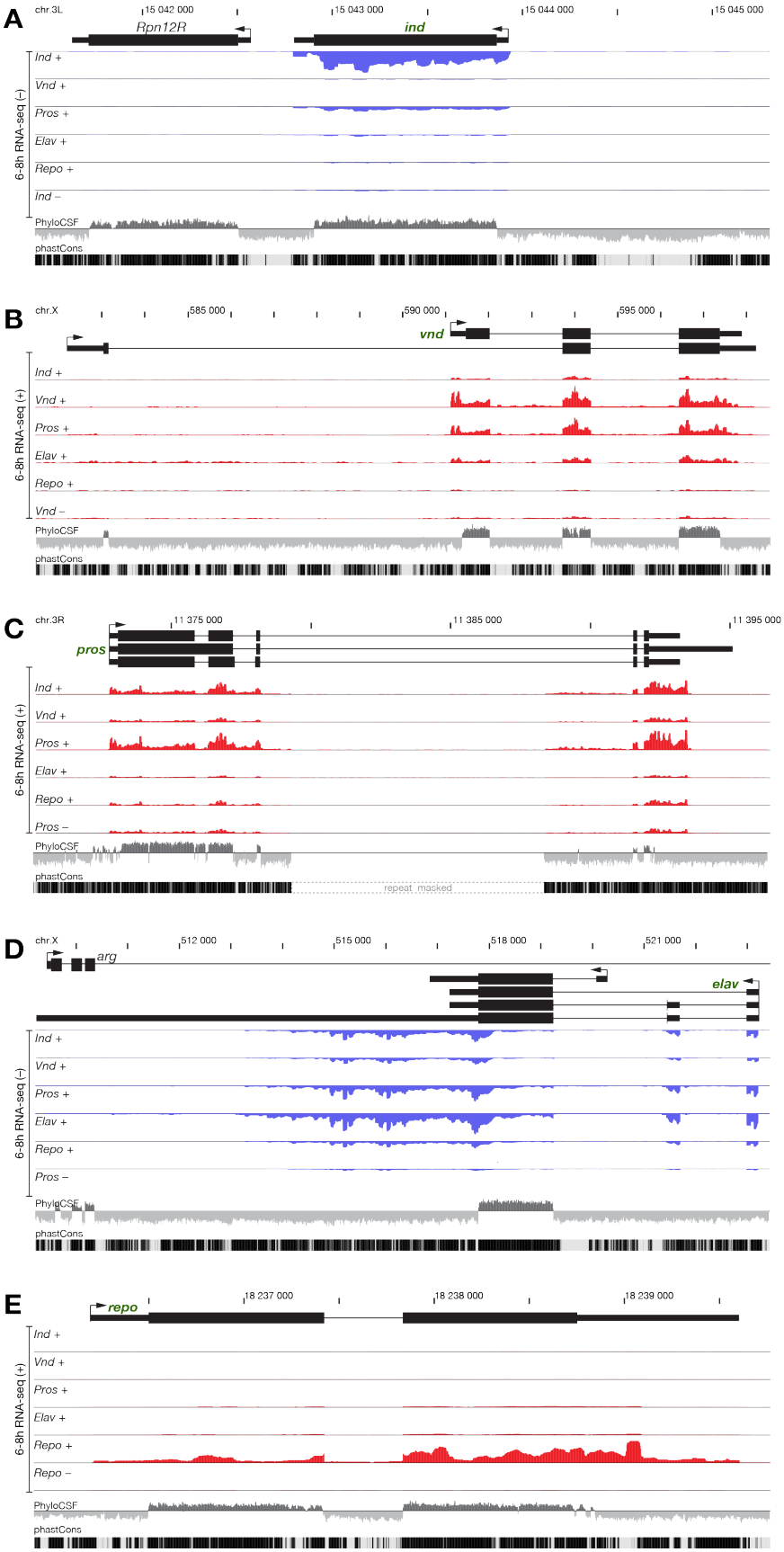
A
chr.3L
15 042 000
15 043 000
15 044 000
15 045 000
Rpn12R
ind
Ind +
Vnd +
Pros +
Elav +
Repo +
Ind –
6-8h RNA-seq (–)
PhyloCSF
phastCons
B
chr.X
585 000
590 000
595 000
vnd
Ind +
Vnd +
Pros +
Elav +
Repo +
Vnd –
6-8h RNA-seq (+)
PhyloCSF
phastCons
C
chr.3R
11 375 000
11 385 000
11 395 000
pros
Ind +
Vnd +
Pros +
Elav +
Repo +
Pros –
6-8h RNA-seq (+)
PhyloCSF
phastCons
repeat masked
D
chr.X
512 000
515 000
518 000
521 000
arg
elav
Ind +
Vnd +
Pros +
Elav +
Repo +
Pros –
6-8h RNA-seq (–)
PhyloCSF
phastCons
E
18 237 000
18 238 000
18 239 000
repo
Ind +
Vnd +
Pros +
Elav +
Repo +
Repo –
6-8h RNA-seq (+)
PhyloCSF
phastCons

Fig. S5: Cell type specific transcriptomes at neurogenic marker genes
(A-E) Genome browser data of cell type specific transcriptomes around marker gene loci. Shown are annotated transcripts (top), RNA-seq coverage on the plus- (red) or minus-strand (blue) in the indicated sorts at 6-8hrs AEL, as well as coding potential as measured by PhyloCSF scores (all frames overlaid), and conservation amongst *Drosophilids* (phastCons). (A) *ind* locus. (B) *vnd* locus. (C) *pros* locus. (D) *elav* locus. (E) *repo* locus.

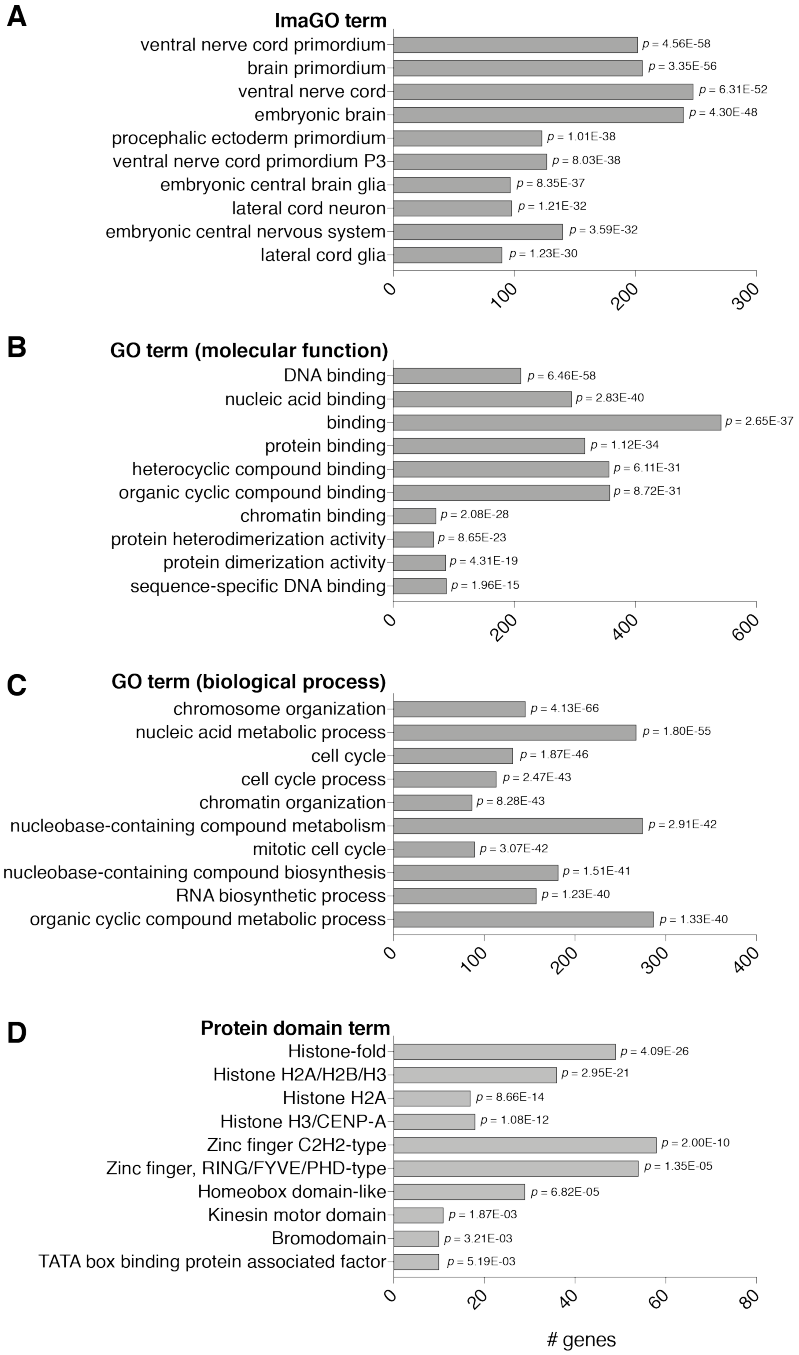

Fig. S6: Annotations of regulated protein-coding genes predict expression and function
Analysis of features of 794 protein-coding genes correlated with known neurogenic genes (Pearson correlation, $r > 0.9$) with Flymine {Lyne:2007jd}. (A) Top ImaGO terms. (B) Top GO terms (molecular function). (C) Top GO terms (biological process). (D) Top protein domain terms. Detailed analysis of all genes can be found in File S2.

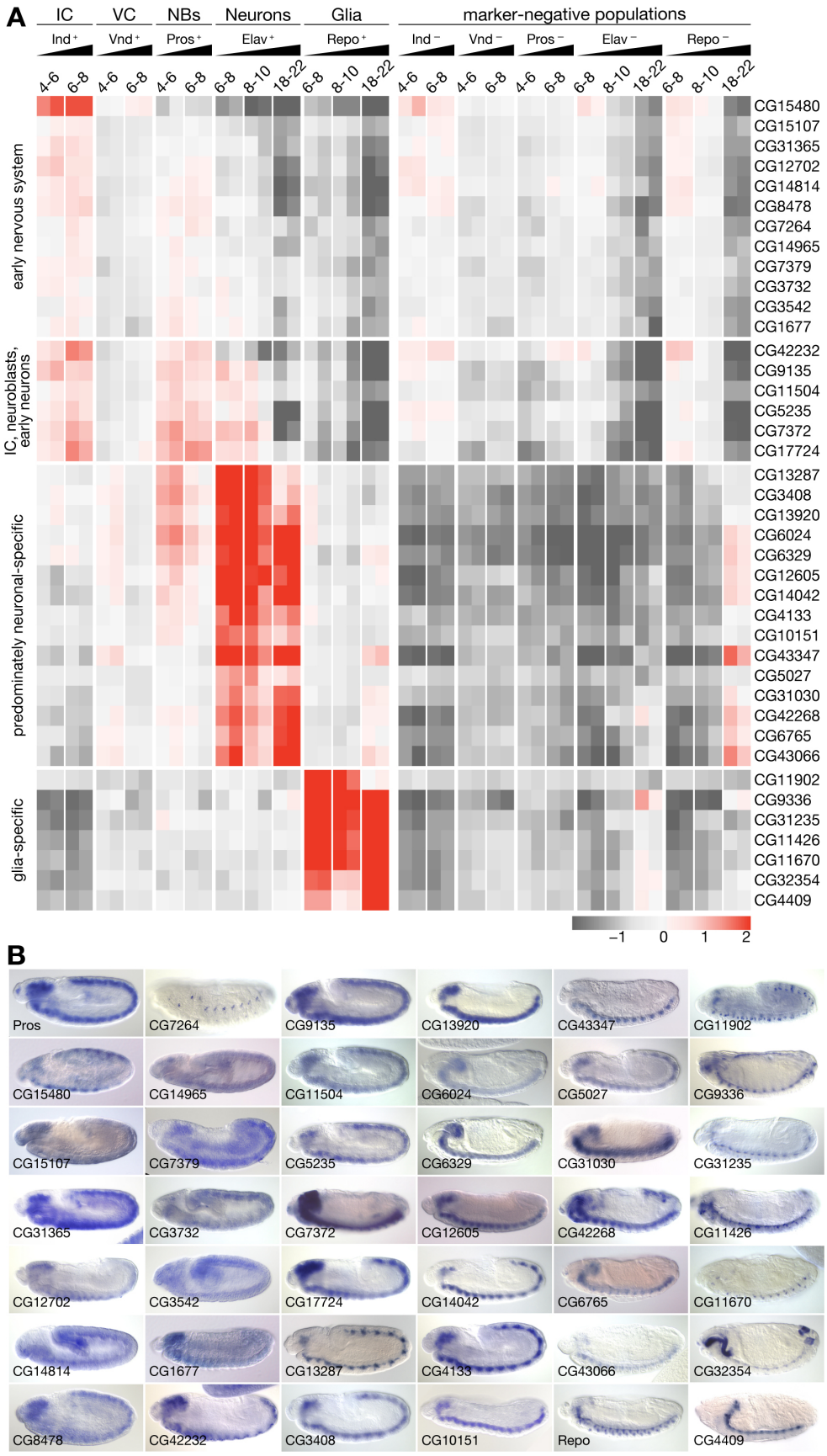
A
IC
VC
NBs
Neurons
Glia
marker-negative populations
Ind+
Vnd+
Pros+
Elav+
Repo+
Ind−
Vnd−
Pros−
Elav−
Repo−
4-6
6-8
8-10
18-22
early nervous system
IC, neuroblasts, early neurons
predominately neuronal-specific
glia-specific
CG15480
CG15107
CG31365
CG12702
CG14814
CG8478
CG7264
CG14965
CG7379
CG3732
CG3542
CG1677
CG42232
CG9135
CG11504
CG5235
CG7372
CG17724
CG13287
CG3408
CG13920
CG6024
CG6329
CG12605
CG14042
CG4133
CG10151
CG43347
CG5027
CG31030
CG42268
CG6765
CG43066
CG11902
CG9336
CG31235
CG11426
CG11670
CG32354
CG4409
−1
0
1
2
B
Pros
CG7264
CG9135
CG13920
CG43347
CG11902
CG15480
CG14965
CG11504
CG6024
CG5027
CG9336
CG15107
CG7379
CG5235
CG6329
CG31030
CG31235
CG31365
CG3732
CG7372
CG12605
CG42268
CG11426
CG12702
CG3542
CG17724
CG14042
CG6765
CG11670
CG14814
CG1677
CG13287
CG4133
CG43066
CG32354
CG8478
CG42232
CG3408
CG10151
Repo
CG4409

Fig. S7: DIV-SortSeq reveals a multitude of undescribed genes expressed with neurogenic spatiotemporal specificity

(A) Heatmap of expression profiles of protein-coding genes with unknown function enriched similarly as at least one marker in Fig. 2B (Pearson correlation, $r > 0.9$). Row mean-centered expression values calculated via variance-stabilizing transformation of gene-level RNA-seq counts (scale = $\log_2$ ratio to row mean). (B) Colorimetric RNA *in situ* hybridization of transcripts of unknown function identified in Fig. S7A. All embryos are shown in lateral orientation. Images obtained from Berkeley *Drosophila* Genome Project (Hammonds et al. 2013; Tomancak et al. 2002; Tomancak et al. 2007).

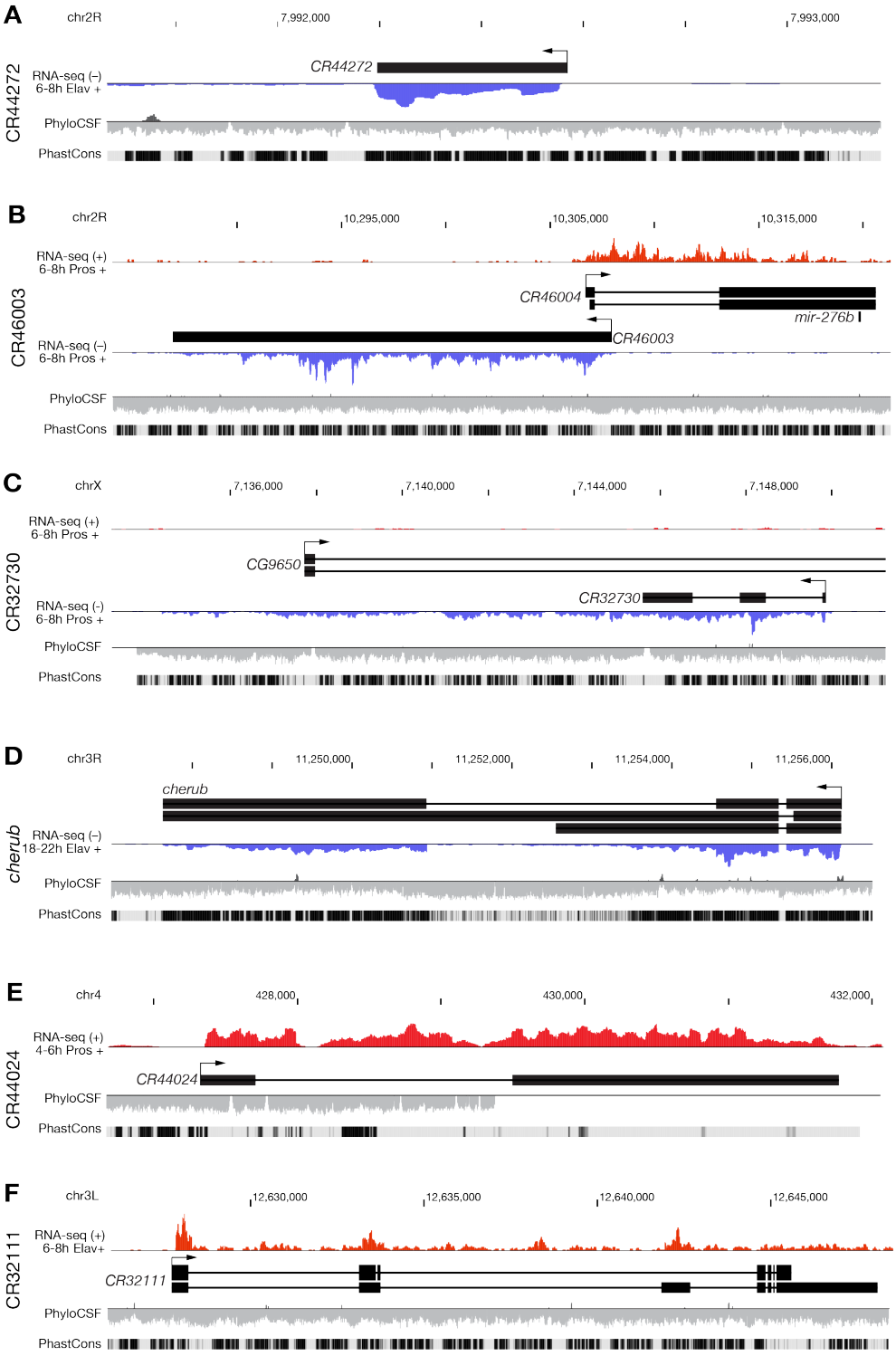
A
chr2R
7,992,000
7,993,000
CR44272
RNA-seq (–)
6-8h Elav +
PhyloCSF
PhastCons
B
chr2R
10,295,000
10,305,000
10,315,000
RNA-seq (+)
6-8h Pros +
CR46004
mir-276b
CR46003
RNA-seq (–)
6-8h Pros +
PhyloCSF
PhastCons
C
chrX
7,136,000
7,140,000
7,144,000
7,148,000
RNA-seq (+)
6-8h Pros +
CG9650
CR32730
RNA-seq (-)
6-8h Pros +
PhyloCSF
PhastCons
D
chr3R
11,250,000
11,252,000
11,254,000
11,256,000
cherub
RNA-seq (–)
18-22h Elav +
PhyloCSF
PhastCons
E
chr4
428,000
430,000
432,000
RNA-seq (+)
4-6h Pros +
CR44024
PhyloCSF
PhastCons
F
chr3L
12,630,000
12,635,000
12,640,000
12,645,000
RNA-seq (+)
6-8h Elav+
CR32111
PhyloCSF
PhastCons

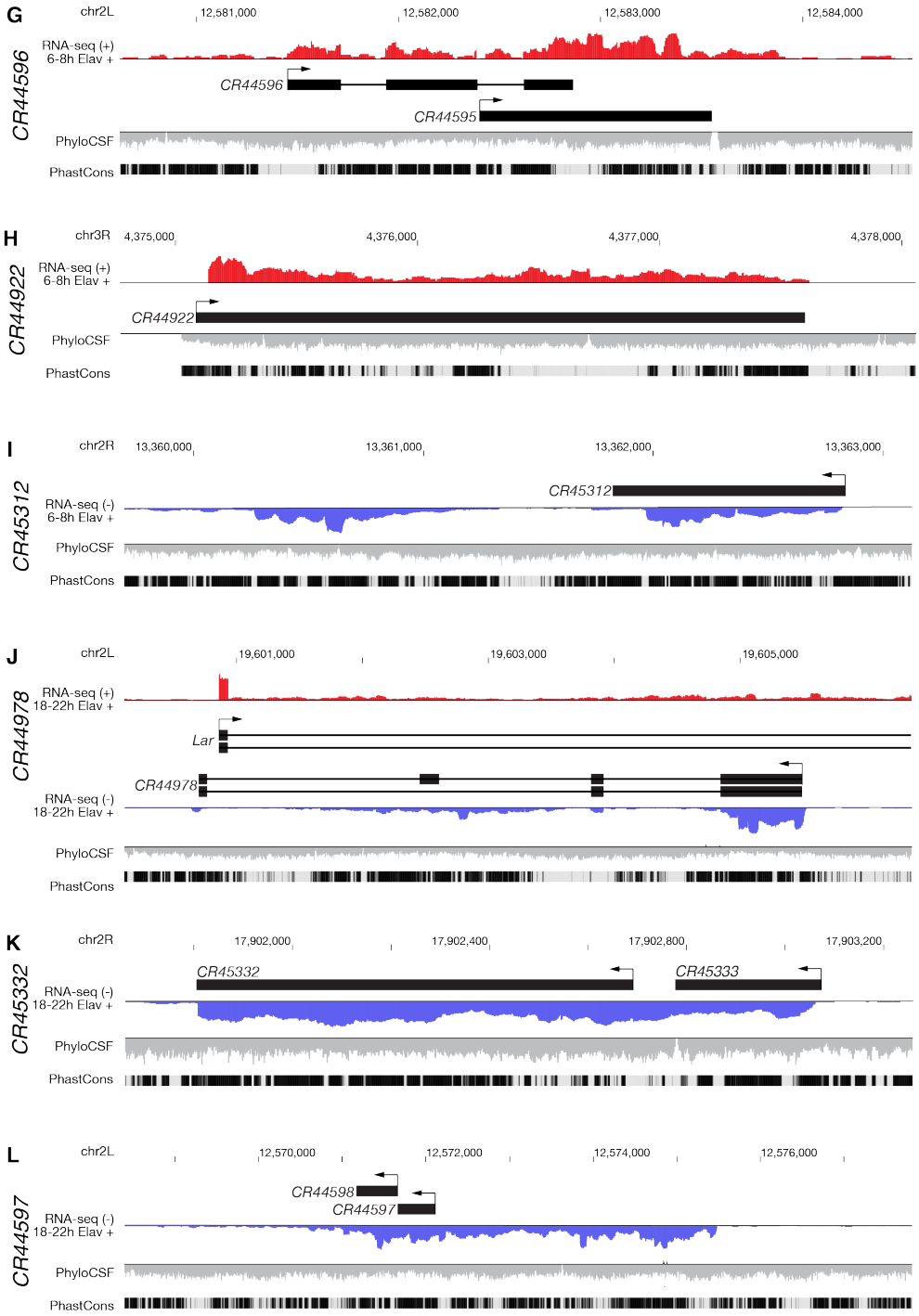

Figure S8: Cell type specific transcriptomes at neurogenic lncRNA loci
Browser images of selected lncRNA loci, display as in Figure S4. (A) *CR44272* locus. (B) *CR46003* and *CR46004* (pri-miR-276b) locus. (C) *CR32730* locus. (D) *cherub* locus. (E) *CR44024* locus. (F) *CR32111* locus. (G) *CR44596* locus. (H) *CR44922* locus. (I) *CR45312* locus. (J) *CR44978* locus. (K) *CR45332* locus. (L) *CR44596* and *CR44597* locus.

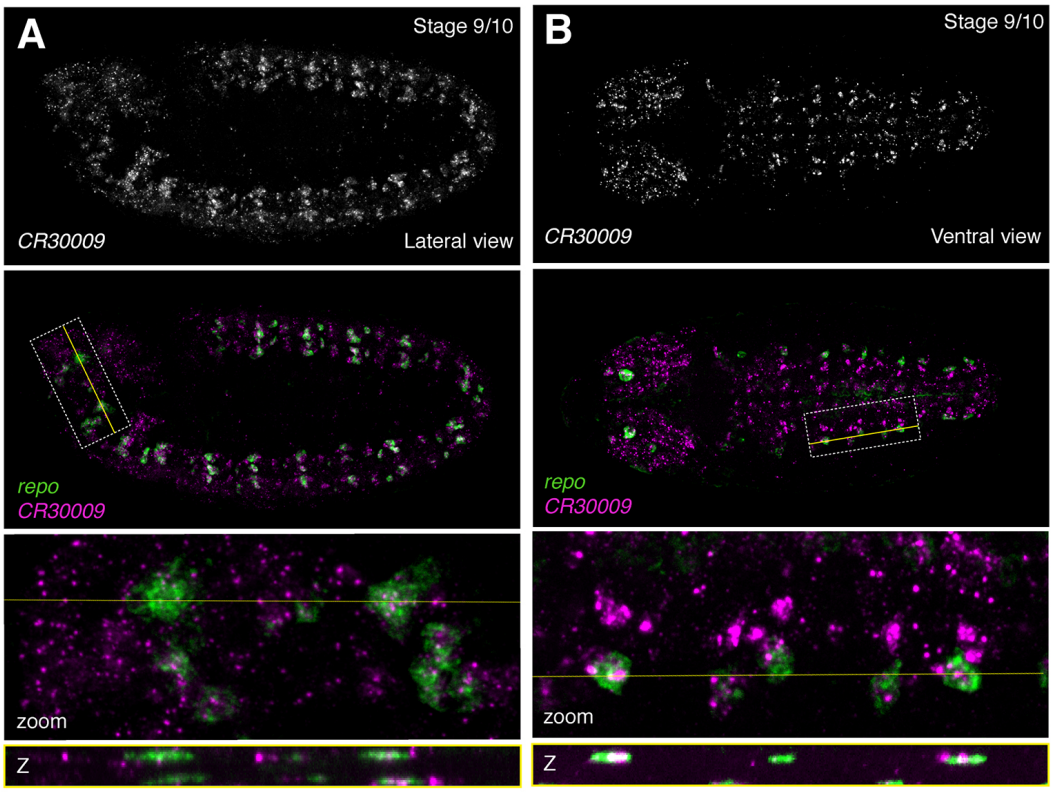

Fig. S10: The lncRNA *CR30009* is expressed in glial subsets in early embryos
RNA fluorescent in situ hybridization (RNA-FISH) against *CR30009* and the glial marker *repo*.
(A) Lateral view, stage 9/10. (B) Ventral view, stage 9/10. Top: *CR30009* alone. Second from top: *CR30009* (magenta) overlaid with *repo* (green). Dashed white box indicates region of interest (ROI) and yellow line indicates Z-slice through ROI. Second from bottom: zoom in of ROI. Bottom: Slice through Z-stack as indicated by yellow line.

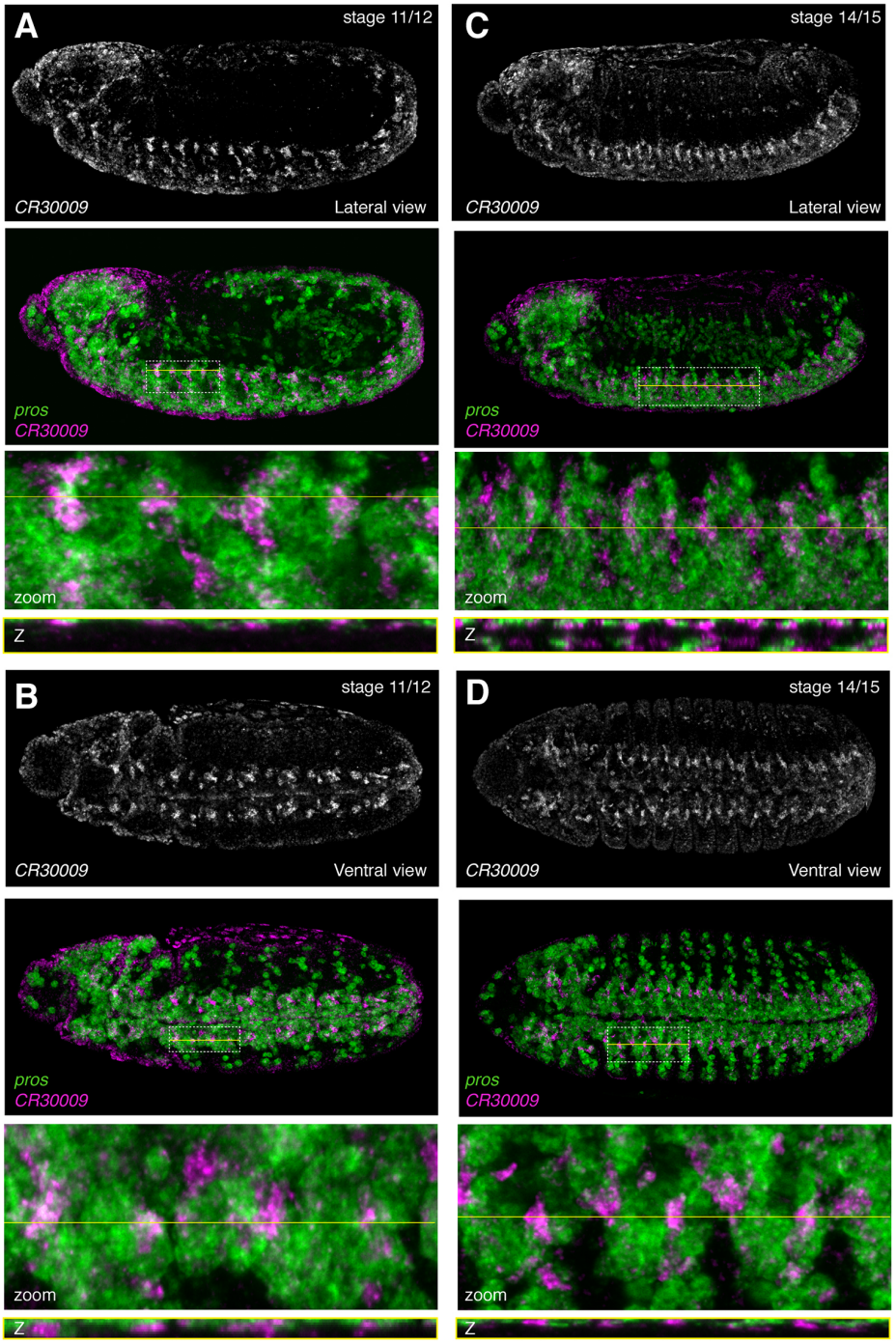

Fig. S11: The lncRNA *CR30009* is expressed in neuroblast subsets
RNA fluorescent in situ hybridization (RNA-FISH) against *CR30009* and the neuroblast marker *pros*. (A) Lateral view, stage 11/12. (B) Lateral view, stage 14/15. (C) Ventral view; stage 11/12. (D). Ventral view; stage 14/15. Top: *CR30009* alone. Second from top: *CR30009* (magenta) overlaid with *pros* (green). Dashed white box indicates region of interest (ROI) and yellow line indicates Z-slice through ROI. Second from bottom: zoom in of ROI. Bottom: Slice through Z-stack as indicated by yellow line.

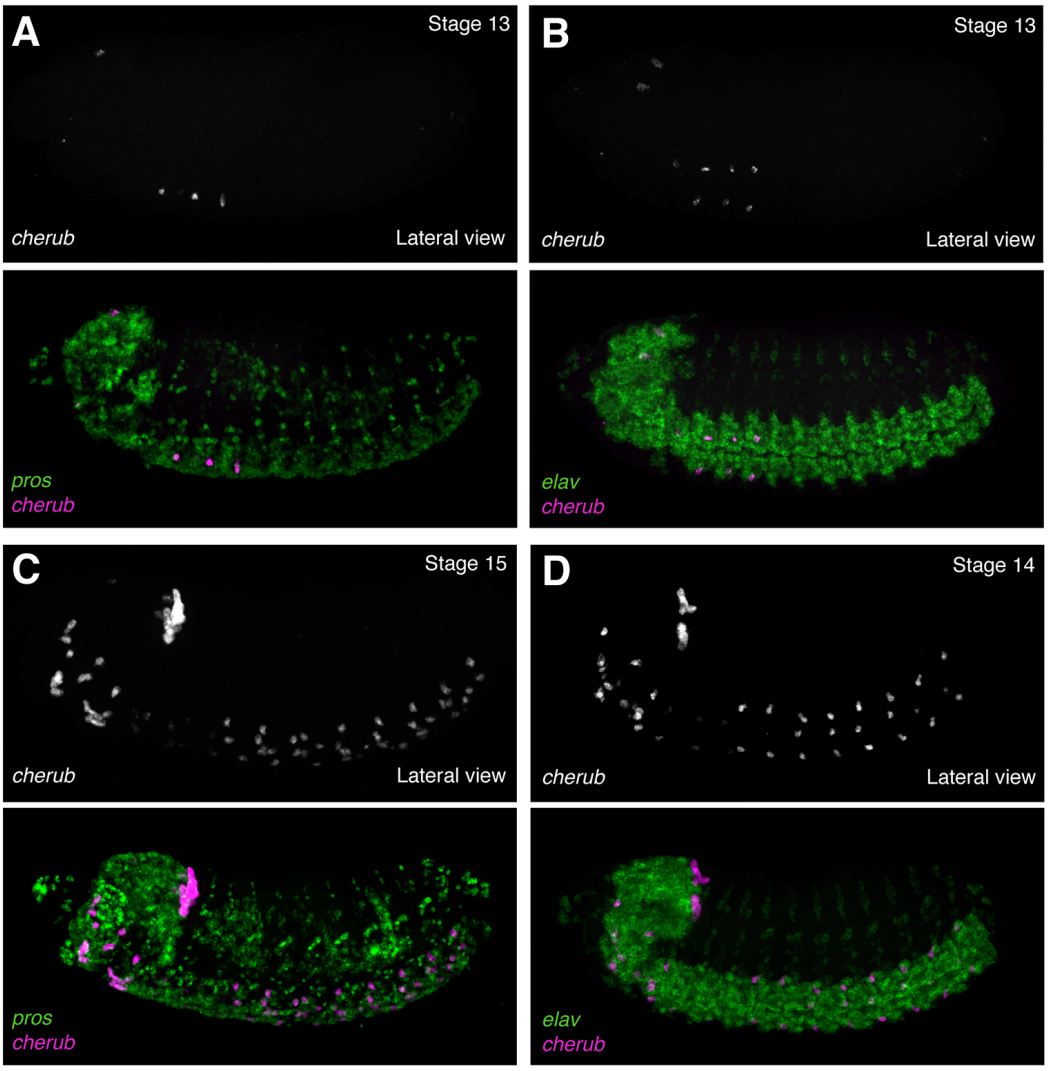

Fig S12: The lncRNA *cherub* is regulated with strict spatiotemporal specificity.
RNA fluorescent in situ hybridization (RNA-FISH) against *cherub*, the neuroblast marker *pros*, and the neuronal marker *elav*. Lateral view. (A) *cherub* with *pros*; stage 13. (B) *cherub* with *elav*; stage 13. (C) *cherub* with *pros*; stage 15. (D) *cherub* with *elav*; stage 14. Top: *cherub* alone. Second from top: *cherub* (magenta) overlaid with marker (green). Dashed white box indicates region of interest (ROI) and yellow line indicates Z-slice through ROI. Second from bottom: zoom in of ROI. Bottom: Slice through Z-stack as indicated by yellow line.

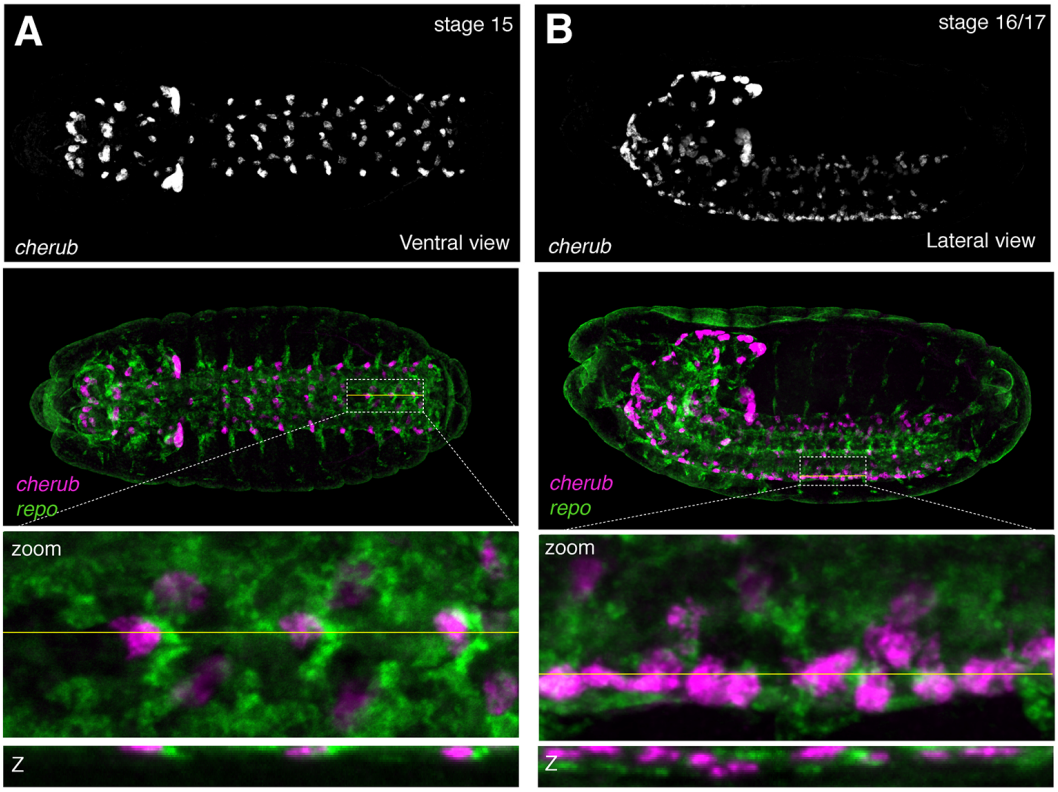

Fig S13: The lncRNA *cherub* is expressed in glial subsets in late embryos
RNA fluorescent in situ hybridization (RNA-FISH) against *cherub* and the glial marker *repo*. (A) Ventral view; stage 15. (B) Lateral view; stage 16/17. Top: *cherub* alone. Second from top: *cherub* (magenta) overlaid with *repo* (green). Dashed white box indicates region of interest (ROI) and yellow line indicates Z-slice through ROI. Second from bottom: zoom in of ROI. Bottom: Slice through Z-stack as indicated by yellow line.

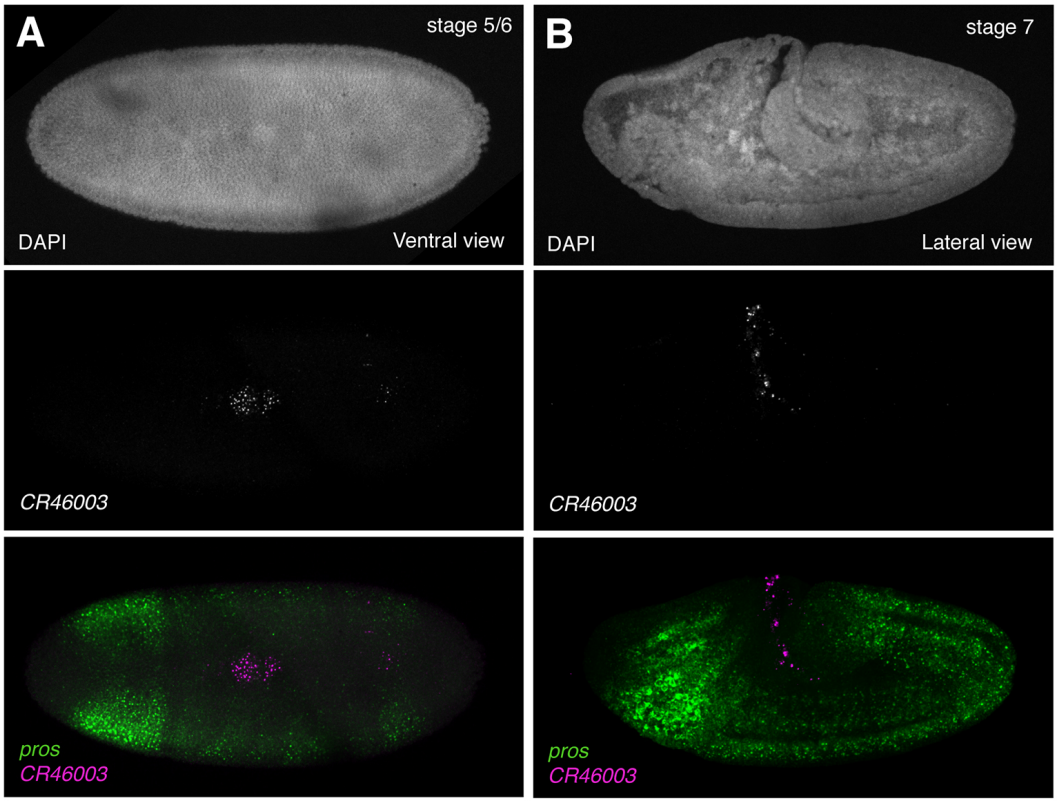

Fig S14: The lncRNA *CR46003* is expressed in very early embryos
RNA fluorescent in situ hybridization (RNA-FISH) against *CR46003* with the neuroblast marker *pros*. (A) Ventral view; stage 5/6. (B) Lateral view; stage 7. Top: DAPI stain. Middle: *CR46003* alone. Bottom: *CR46003* (magenta) overlaid with *pros* (green).

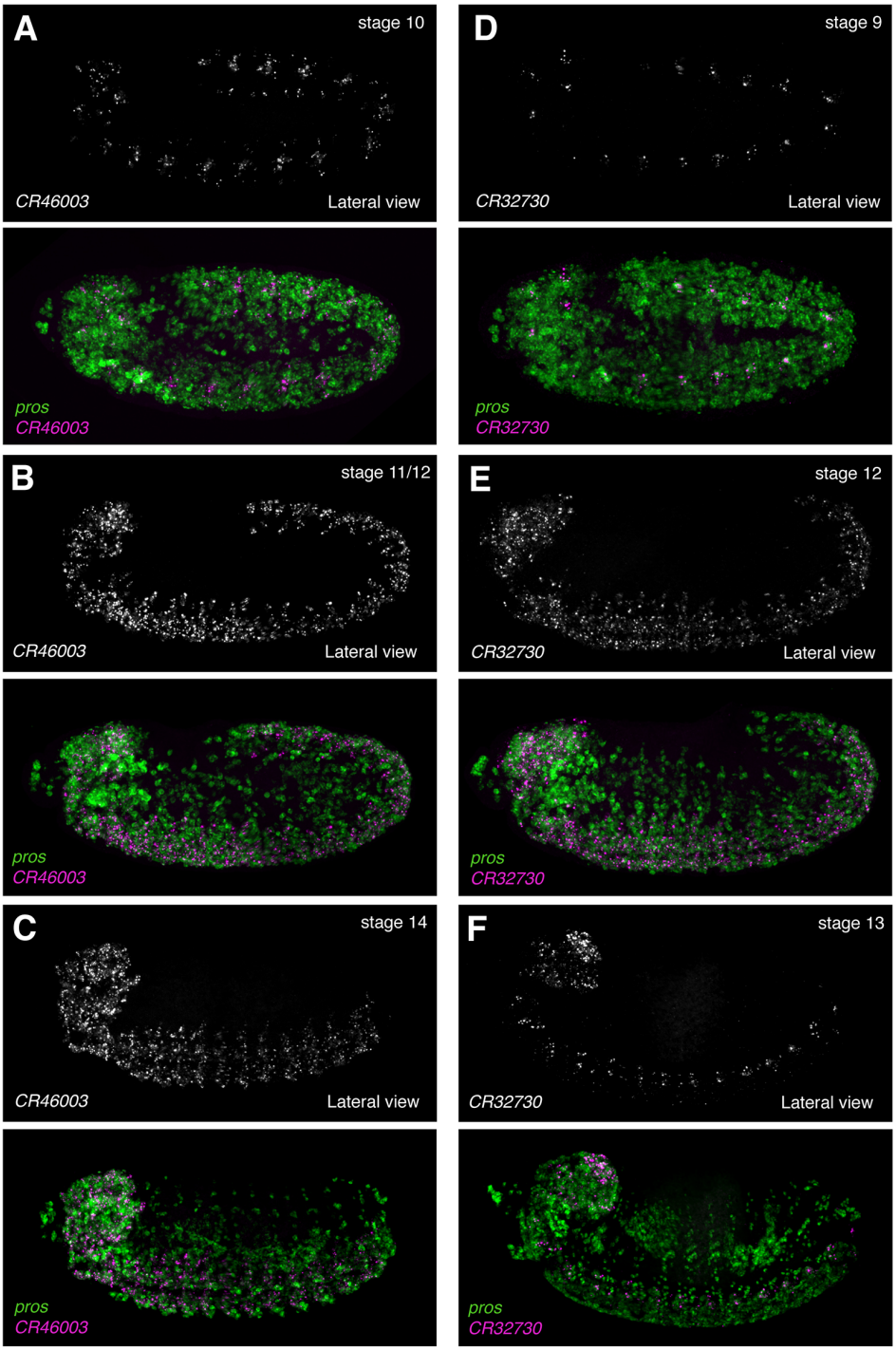

Fig S15: The lncRNAs *CR46003* and *CR32730* are expressed with similar spatiotemporal specificity.

RNA fluorescent in situ hybridization (RNA-FISH) against *CR46003* and *CR32730* together with the neuroblast marker *pros*. Lateral view. (A) *CR46003*; stage 10. (B) *CR46003*; stage 11/12. (C) *CR46003*; stage 14. (D) *CR32730*; stage 9. (E) *CR32730*; stage 12. (F) *CR32730*; stage 13. Top: lncRNA alone. Second from top: lncRNA (magenta) overlaid with *pros* (green).

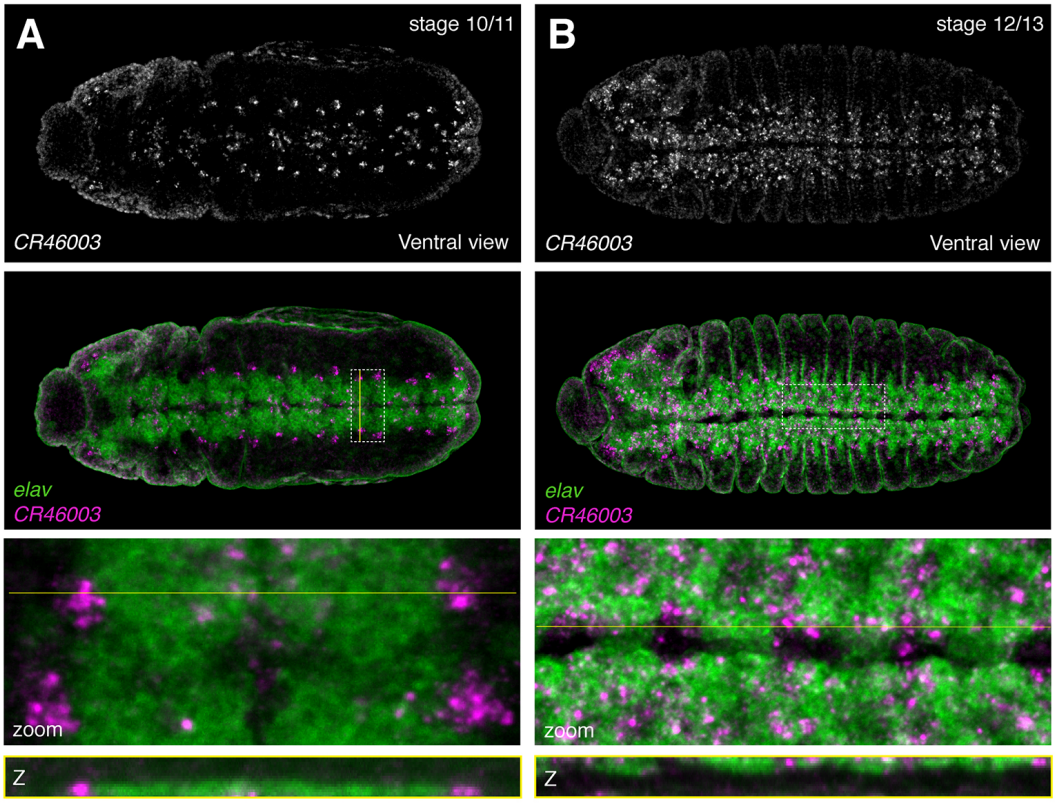

Fig S16: The lncRNA *CR46003* is expressed in neuronal subsets

RNA fluorescent in situ hybridization (RNA-FISH) against *CR46003* with the neuronal marker, *elav*. Ventral view. (A) Stage 10/11. (B) Stage 12/13. Top: *CR46003* alone. Second from top: *CR46003* (magenta) overlaid with *elav* (green). Dashed white box indicates region of interest (ROI) and yellow line indicates Z-slice through ROI. Second from bottom: zoom in of ROI. Bottom: Slice through Z-stack as indicated by yellow line.

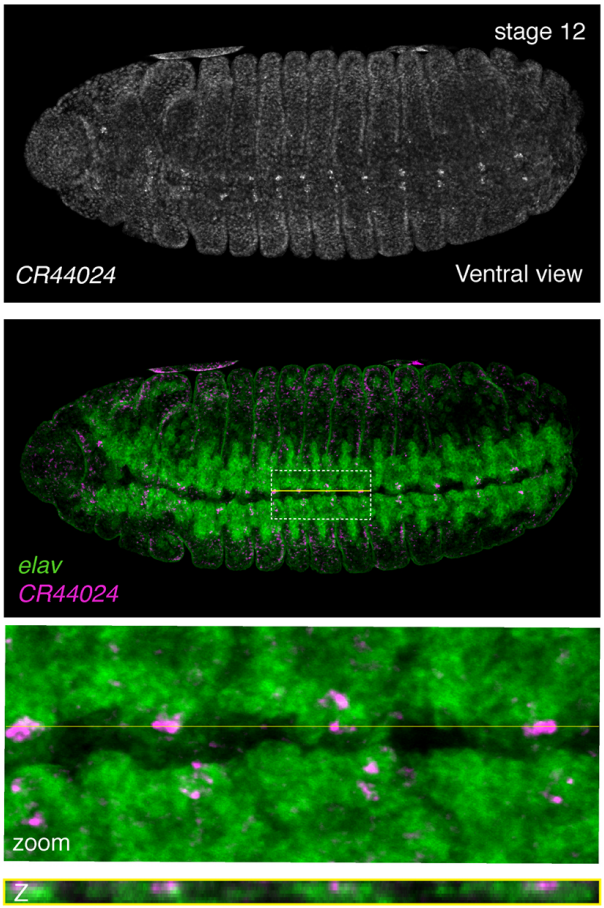

Fig S17: The lncRNA *CR44024* is expressed from stage 12 in neuronal subsets of the ventral nerve cord.
RNA fluorescent in situ hybridization (RNA-FISH) against *CR44024* with the neuronal marker, *elav*. Ventral view, stage 12. Top: *CR44024* alone. Second from top: *CR44024* (magenta) overlaid with *elav* (green). Dashed white box indicates region of interest (ROI) and yellow line indicates Z-slice through ROI. Second from bottom: zoom in of ROI. Bottom: Slice through Z-stack as indicated by yellow line.

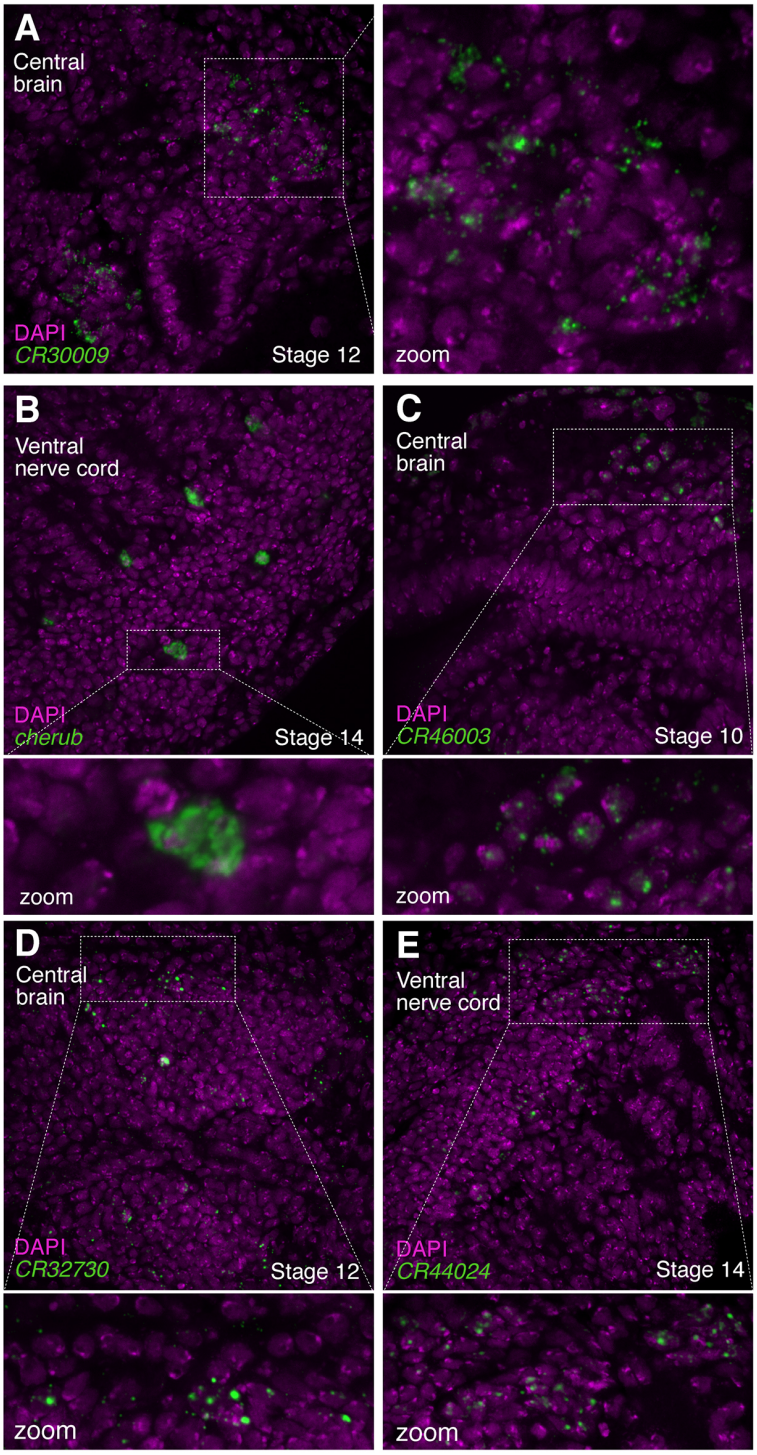

Fig S18: LncRNAs exhibit varying patterns of subcellular distribution

RNA fluorescent in situ hybridization (RNA-FISH) against lncRNAs (green) overlaid with the nucleic acid marker, DAPI (magenta). (A) *CR30009*; central brain, stage 12. (B) *cherub*; ventral nerve cord, stage 14. (C) *CR46003*; central brain, stage 10. (D) *CR32730*; central brain, stage 12. (E) *CR44024;* ventral nerve cord, stage 14. (A) Left panel: Dashed white box indicates region of interest (ROI). Right panel: zoom in of ROI. (B-E) Top panel: Dashed white box indicates region of interest (ROI). Bottom panel: zoom in of ROI.

5. Supplementary References

Barolo, S., Castro, B. & Posakony, J.W., 2004. New Drosophila transgenic reporters: insulated P-element vectors expressing fast-maturing RFP. *BioTechniques*, 36(3), pp.436–40– 442.

Bhatt, D.M. et al., 2012. Transcript dynamics of proinflammatory genes revealed by sequence analysis of subcellular RNA fractions. *Cell*, 150(2), pp.279–290.

Hrvatin, S. et al., 2014. MARIS: Method for Analyzing RNA following Intracellular Sorting K. Aalto-Setala, ed. *PLoS ONE*, 9(3), pp.e89459–6.

Karaiskos, N. et al., 2017. The Drosophila embryo at single-cell transcriptome resolution. *Science*, 358(6360), pp.194–199.

Markstein, M. et al., 2004. A regulatory code for neurogenic gene expression in the Drosophila embryo. *Development*, 131(10), pp.2387–2394.

Pawlicki, J.M. & Steitz, J.A., 2008. Primary microRNA transcript retention at sites of transcription leads to enhanced microRNA production. *The Journal of cell biology*, 182(1), pp.61–76.

Rosner, M. & Hengstschläger, M., 2012. Detection of cytoplasmic and nuclear functions of mTOR by fractionation. *Methods in molecular biology (Clifton, N.J.)*, 821(Chapter 8), pp.105–124.

Rubin, G.M. & Spradling, A.C., 1982. Genetic transformation of Drosophila with transposable element vectors. *Science*, 218(4570), pp.348–353.

Schmittgen, T.D. & Livak, K.J., 2008. Analyzing real-time PCR data by the comparative C(T) method. *Nature Protocols*, 3(6), pp.1101–1108.

Shechner, D.M. et al., 2015. Multiplexable, locus-specific targeting of long RNAs with CRISPR-Display. *Nature Methods*, 12(7), pp.664–670.

Stapleton, M. et al., 2002. The Drosophila gene collection: identification of putative full-length cDNAs for 70% of D. melanogaster genes. *Genome Research*, 12(8), pp.1294–1300.

Vandesompele, J. et al., 2002. Accurate normalization of real-time quantitative RT-PCR data by geometric averaging of multiple internal control genes. *Genome biology*, 3(7), p.RESEARCH0034.